INVESTIGATION OF DOSIMETRIC AND THERMOLUMINESCENCE PROPERTIES OF CaF2:Mn (TLD-400)

M. Sc. Thesis

in

Engineering Physics

University of Gaziantep

Supervisor

Asst.Prof.Dr. METİN BEDİR

BY

AYŞE SİBEL SÖKÜCÜ

JULY 2007

GAZİANTEP UNIVERSITY
GRADUATE SCHOOL OF
NATURAL & APPLIED SCIENCES
Department of Engineering Physics

Name of the thesis: Investigation of Dosimetric and Thermoluminescence Properties of CaF_2:Mn (TLD-400)
Name of the student: Ayşe Sibel SÖKÜCÜ
Exam date: 06.07.2007

Approval of the Graduate School of Natural and Applied Sciences

Prof. Dr. Sadettin ÖZYAZICI
Director

I certify that this thesis satisfies all the requirements as a thesis for the degree of Master of Science/Doctor of Philosophy.

Prof. Dr. Beşire GÖNÜL
Head of Department

This is to certify that we have read this thesis and that in our opinion it is fully adequate, in scope and quality, as a thesis for the degree of Master of Science/Doctor of Philosophy.

Assist. Prof. Dr. Metin BEDİR
Supervisor

Examining Committee Members	signature
Assoc. Prof. Dr..A. Necmeddin YAZICI	_____
Assoc. Prof. Dr. Yaşar GÜNDOĞDU	_____
Asst. Prof. Dr. R. Güler YILDIRIM	_____
Asst. Prof. Dr. Mustafa ÖZTAŞ	_____
Asst. Prof. Dr. Metin BEDİR	_____

ABSTRACT

INVESTIGATION OF DOSIMETRIC AND THERMOLUMINESCENCE PROPERTIES OF CaF_2:Mn (TLD-400)

SÖKÜCÜ Ayşe Sibel

M. SC., in P. E. University of Gaziantep

Supervisor: Asist.Prof.Dr. Metin BEDİR

July 2007, 53 pages

The additive dose (AD), $T_m(E_a)$–T_{stop}, repeated initial rise (RIR), peak shape (PS), and computerized glow curve deconvolution (CGCD) methods were used to analyze the thermoluminescent (TL) dosimetric glow peak of CaF_2:Mn after β-irradiation between the dose level D=0.015 Gy and D=110 Gy. The activation energies found with the IR and PS methods yield very close values after the cleaning of low temperature satellite peaks from the dosimetric glow peak by increasing stopping temperature in the T_m–T_{stop} experiment. The influence of heating rates on the response of dosimetric glow peak of CaF_2:Mn was also studied by the peak height and peak area methods using CGCD technique. It was observed that the peak intensities and total area of glow peak decrease continuously with increasing heating rate.Another dosimetric characteristic which is the dose response of this peak was also examined by peak height and area methods.

Keywords: Thermoluminescence; CaF_2:Mn; TLD-400; Kinetic parameters; Dose response; Heating rate

ÖZET

CaF_2:Mn NİN DOZİMETRİK VE TERMOLUMİNESANS ÖZELLİKLERİNİN ARAŞTIRILMASI

Beta ışını ile 0,015 Gy ile 110 Gy arası ışınlanmış CaF_2:Mn termoluminesans dozimetresinin ışıldama eğrisi Doz Ekleme (AD), $T_m(E_a)$–T_{stop}, Tekrarlanan İlk Yükselme (RIR), Işıldama Tepesi Şekli (PS) ve Bilgisayar İle Işıldama Eğrisi Ayrışımı (CGCD) metotları kullanılarak analiz edildi. T_m–T_{stop} deneyinde T_{stop} sıcaklığının yükselmesi sonucu dozimetrik ışıldama tepesinin düşük sıcaklık tarafındaki küçük uydu tepelerinin temizlenmesinin ardından IR ve PS ile bulunan aktivasyon enerjileri oldukça yakın sonuçlar vermiştir. Dozimetrik ışıldama tepesinin tepkisi üzerinde sıcaklık artış oranı maksimum şiddet ve CGCD metodu kullanarak tepe alanının bulunması ile çalışıldı. Sıcaklık artış oranı ile dozimetrik ışıldama tepesinin maksimum şiddetinin ve tepe alanlarının her ikisinin de azaldığı görüldü. Bu dozimetrik ışıldama tepesinin doz-cevap ilişkisi yine maksimum şiddet ve tepe alanı yönetimi ile araştırıldı.

Anahtar kelimeler: Termoluminesans; Ca:F_2:Mn; TLD(400); Kinetik parametre; dose cevap; Sıcaklık artış oranı.

ACKNOWLEDGEMENT

During the writing of this thesis, the author received many helps from people to whom she would like to thank. First of all I would like to thank my supervisor Assist. Prof. Dr. Metin BEDİR helps and advices during the preperation of this thesis. I am truly grateful for the encouragement and consideration of him. Secondly, I wish to thank Assoc. Prof. Dr. Necmeddin YAZICI. I have benefited from the aid and advice of him during the writing and preparation of this thesis. I would like to thank my gratitude the research assistances and other personnel at the Department of Engineering Physics for their kind help and friendships.

TABLE OF CONTENT

LIST OF FIGURES

LIST OF TABLES

CHAPTER 1

INTRODUCTION

Thermoluminescence (TL) or thermally stimulated luminescence is the emission of light during heating of solid sample (insulator or semiconductor), previously excited by radiation. The TL material absorbs energy during exposure to radiation (ionising, visible light, UV etc.) and stores this energy until heated. The intensity of emitted light as a function of temperature is the thermo luminescence glow curve. Usually the heating rate is constant, and therefore the glow curve is often shown in the literature as the TL intensity as a function of the time of the measurement cycle or the channel number instead of the temperature. In this case it is advisable to show also the time-temperature profile in addition to the glow curve [1].

The theoretical explanation of thermo luminescence is based on the electron band theory. TL materials are insulators or semiconductors with a crystalline structure. According to the simplest model, the one trap-one centre model, in an ideal crystal the electrons occupy the valence bands, which are separated from the conduction band by the so-called forbidden band gap. In real crystals various defects occur as a consequence of ionizing radiation or of impurities in the lattice. In both cases the electrons can possess “forbidden” energies. The excitation of electrons from the valence band to the conduction band may occur as a result of irradiation, while holes remain in the valence band. Some of the electrons and holes can recombine under emission of light (radioluminescence), while the others will be trapped at the level LT in the “forbidden” energy gap [1].

Thermoluminescence (TL) method is relatively complex process since it involves a trap and a luminescence center. When an insulator or semiconductor is exposed to ionizing radiation at room or at low temperature, electrons are released

from the valence band to the conduction band. This leaves a hole in the valence band. Both types of carriers become mobile in their respective bands until they recombine or until they are trapped in lattice imperfections in the crystalline solids. These lattice imperfections play very crucial role in the TL process. The trapped electrons may remain for a long period when the crystals are stored at room temperature. They can be released due to the sufficient energy given to the electron when the crystal is heated. These electrons may move in the crystalline solid until they recombine with suitable recombination centers that contain hole with the emission of TL light. This process of light emission by stimulation from a crystalline solid after irradiations is called as "thermally stimulated process" or simply "thermoluminescence".

In this statement it can be found the three essential ingredients necessary for the production of thermoluminescence. Firstly, the material must be an insulator or a semiconductor – metals do not exhibit luminescent properties. Secondly, the material must have at some time absorbed energy during exposure to radiation. Thirdly, the luminescence emission is triggered by heating the material. In addition, there is one important property of thermoluminescence which cannot be inferred from this statement as it stands at present. It is a particular characteristic of thermoluminescence that, once heated to excite the light emission, material can not be made to emit thermoluminescence again by simply cooling the specimen and reheating. In order to re-exhibit luminescence the material has to be re-exposed to radiation, where upon raising the temperature will once again procedure light emission. The fundamental principles which govern the production of thermoluminescence are essentially the same as those which govern all luminescence process, and in this way thermoluminescence is merely one of a large family of luminescence phenomena [2].

Thermoluminescence dosimeters (TLDs) based on CaF_2 have been highly attractive for radiation dosimetry in both natural (fluorite) and synthetic forms. Especially, Mn^{2+}-doped CaF_2 has been used over the past four decades as an important thermoluminescent (TL) dosimetry due to its high sensitivity (compared to TLD-100) to doses as low as 50 μGy and a simpler glow curve structure. Therefore, it has found widespread use in the field of environmental and personnel radiation dosimetry, despite some problems associated with batch-to-batch irreproducibility, anomalous fading, degradation during re-use, perennial zero dose problem and its poor energy response resulting from its high effective atomic number compared with

tissue. The lack of tissue equivalence precludes its regular use as a personal dosimeter, but its higher sensitivity make it an excellent environmental dosimetric material since exposure time in the field can be reduced accordingly [3,4]. In the zero dose problems, TLDs without exposure to radiation read a dose of ≈0.1 mGy or more above the natural background level when stored in the dark (dependent on the prior exposure history of the sample). Over the past years much effort has been spent to identify the cause of this chronic problem and it was observed that the peak near 390 ^{o}C has a vital role on the dosimetric performance of this material [5]. Unless this peak is thoroughly cleaned either by heating the TLDs beyond 400 ^{o}C, the dosimetric peak near 290 ^{o}C is regenerated without further exposure to radiation and therefore the TLDs will produce a zero dose problem depending upon the previous dose and elapsed time after readout. On the other hand, when the high-temperature traps near and above 400 ^{o}C are completely depleted, optically or thermally, this problem is removed. Moreover, laser cleaning of this trap is preferred. Because, this process, being performed at room temperature, will not reduce the sensitivity of the TLDs which might happen with heating above 400 ^{o}C. Another way to minimize the zero dose problem is the lowering the concentration of Mn^{2+} in the material. This would reduce the formation of Mn^{2+} pairs which are through to be the origin of the center responsible for the zero dose problems. A survey of the literature has indicated that there are many attempts to understand the thermoluminescence mechanism and dosimetric properties of CaF_2:Mn during last forty years. As a result of these investigations, very different approaches have been used and different models were suggested to explain its TL mechanism [6-9]. Although many investigations of the TL properties of CaF_2:Mn have been performed, the kinetic parameters and some of the dosimetric characteristics such as dose response and fading behaviors of glow peaks are not studied in detail yet.

An early attempt to analyze the number of glow peaks and their kinetic parameters in CaF_2:Mn between room temperature and 400 ^{o}C was studied and concluded by Paul W. Levy *et al* [10,11]. They have indicated that at first sight the main glow peak of this material appears to consist of a single first-order glow peak at around 290 ^{o}C which is very stable at room temperature. A fit of this peak using a single first-order peak yields E_a=1.05 eV and s=6.73x10^{7} s^{-1}, while an analysis using Chen's shape factors yields E_a=0.95 eV and s=1.87x10^{7} s^{-1}. However, the fit obtained is poor and better results are obtained using a more general, intermediate

order. Such an analysis yields E_a=1.04 eV and s=6.3x10^7 s^{-1}, although the fit is still not perfect, especially in the low temperature, initial rise region. Furthermore, the same authors were shown that the general, intermediate order kinetic analysis yields E_a=1.38-1.4 eV (s=1.4x10^{11}-2.8x10^{11} s^{-1}) for samples that have been post-irradiation annealed in some fashion. This clearly suggests that the glow curve is caused by either several closely spaced (in energy) traps, or results from charge released from a continuous distribution of traps [12]. The peak numbers in TLD-400 and their positions were also determined by Drazic (1986) with the experimental method based on annealing studies [13] and it was confirmed that the main glow peak was composed of three peaks with the kinetic parameters shown in Table 1.1.

Table 1.1 Glow peaks and their kinetic parameters used in calculations CaF_2:Mn (IJS TLD-05) TLDs determined by Drazic et al

Peak 1	E_a (eV)	s (cm^{3}s^{-1})	T_m (^{o}C)
1	0.80	6.5x10^7	220
2	0.86	4.4x10^7	265
3	0.94	6.5x10^7	301

On the other hand, another group author [14,15] has indicated that the number and position of TL peaks in CaF_2 depends solely on Mn-concentration and distribution of it in the crystal lattice. This group was indicated that as the Mn-content of CaF_2:Mn increased from 0 to 3%, a set of originally well-separated multi-peaked TL spectra would gradually incorporated into a single TL peak. These observations were also supported by measurements of PTTL. In fact, the PTTL data strongly suggest that the CaF_2:Mn glow curve is made up of at least two, closely overlapping, but discrete TL peaks, rather than a single peak caused by a continuous distribution of activation energies. These results implied that the radiation-induced defects of these overlapped peaks were all Mn-related. As a result, one may summarized by saying that the activation energy for TL emission is ≈1 eV and that the glow peak is not elementary and it appears to be made up of several, closely spaced, discrete TL peaks if the manganese content in CaF_2 is about 3 mol% in the melt.

The dosimetric characteristics of any TL material mainly depend on the sensitivity, energy response and the kinetic parameters quantitatively describing the trapping–emitting centers responsible for the TL emission. Thus, a reliable dosimetric study of a thermoluminescent material should be based on a good knowledge of its kinetic parameters. For example, the simultaneous estimation of the dose rate and the time elapsed since exposure are closely related to the position of the trapping levels within the band gap, and therefore it is necessary to have a good knowledge of these parameters. There are various methods for evaluating the trapping parameters from TL glow curves [2]. When one of the glow peaks is highly isolated from the others, the experimental methods such as initial rise, various heating rates, and peak shape methods are suitable methods to determine them. However, in most materials, the glow curve consists of several overlapping peaks, which is also the case in CaF_2:Mn. When more than one glow peak is present in the glow curve, there are essentially two ways to obtain these parameters: the first is to isolate each individual TL peak from the others using partial thermal annealing treatment and the other is to make a complete glow curve analysis using deconvolution [16]. Therefore the AD, $T_m(E_a)$–T_{stop}, RIR and PS methods along with the deconvolution method have been used to analyze the glow curves of CaF_2:Mn (TLD-400) [2,16-19].

CHAPTER 2

THEORY OF THERMOLUMINESCENCE

2.1. Basic Concepts of Thermoluminescence in Solids

The phenomenon thermoluminescence (TL) has been known for a long time. The first application of this phenomenon for dosimetric purposes was from Daniel et al. [20]. Since then much research has been carried out for a better understanding and improvement of the material characteristics as well as to develop new TL materials. Nowadays, thermoluminescence dosimetry (TLD) is a well-established dosimetric technique with applications in areas such as personnel, environmental and clinical dosimetry.

Thermoluminescence is the physical phenomenon in which a solid sample absorbs energy while irradiated at a given temperature, and releases this energy in the form of light while heating the sample. The emitted light is recorded as intensity vs. temperature in the shape of one or more TL peaks. Under favorable conditions, the emitted TL light intensity is proportional to the absorbed dose, and thus, using an appropriate calibration, one can evaluate the applied dose in the given radiation field. The TL signal may be the intensity at the maximum or the area under the TL glow peak, which are usually nearly proportional to each other. In "regular" dosimetric applications, one can choose an appropriate material with reproducible results in repeated measurements, linear dose dependence for the kind of radiation in question as well as dose-rate independence and long time stability.

Thermoluminescence is an established method for radiation dosimetry as well as retrospective dosimetry. In spite of its great success, different difficulties are associated with its application. These include anomalous fading, changes in the properties of the sample due to its heating in the readout phase, including a sensitization due to the combined effect of irradiation and heating and non-linear

dose dependence observed in some potential dosimetric materials. Another point is that once the sample is heated during the read-out, the TL signal is erased; this is of help for re-use of the sample, but prevents a repeated reading of the measured quantity. The alternative of using optically stimulated luminescence has become very popular in recent years. Here, the ill effects associated with the heating of the sample are avoided. Also, the possibility of reading out the sample several times exists. This can be done by using short pulses of stimulating light, which deplete only a small part of the trapped charge carriers. The present work points out some difficulties that may take place with OSL. These include a possible superlinearity in the dose dependence as well as dose-rate dependence. Also is discussed the difference between pulsed and integral OSL signals.

Thermoluminescence dosimeter (TLD) is a thermoluminescent phosphor in which ionizing radiation causes trapping of freed electrons (or holes) at lattice defects in the crystal structure. Thermoluminescence (TL) is the emission of light happening when electrons (or holes) are released from the traps and return to stable states; the escape probability is greatly increased by raising phosphor temperature. If TL emission is detected and plotted as a function of time during TLD temperature linear growing, a curve is obtained named Glow Curve (GC) exhibiting several peaks, eventually not resolved, and corresponding to the various energies of the emptied traps. The amplitude of each peak, or the subtended area, is approximately proportional to the trap population and consequently, in the case of a single radiation field, to the absorbed dose. The population probabilities of the various traps are different for different radiation kinds, and therefore the GC shape is different too. Therefore, in mixed radiation fields, the absorbed dose cannot be promptly determined. In literature, several methods can be found, mainly for health physics purpose, for dose determination in mixed fields by means of coupled TLDs employment. However, for measurements at therapy dose levels, more troubles arise, and further research is needed.

TLD Dosimeters are one of the most advanced applications of Thermoluminescent Detectors. The reason for this is that, according to the new 10 CFR Part 20 Guidelines of the US NRC, modern TLD Dosimeters measure the Skin Dose, Eye Dose and Deep Dose specified in this regulation, in addition to the dose due to other nuclear particles. Thus, modern TLD Dosimeters consist of at least four separate TL detectors, which are shielded by materials of various compositions and

thicknesses, to allow for discrimination of photon energies and the nature of the incident radiation**.**

As a result of irradiation, some solid substances undergo changes in some of their physical properties. These changes amount to storage of the energy from the radiation. Since the energy is stored, these materials can be used for dosimeters. The property of thermoluminescence (thermo means heat and lumen means light) of some materials is the main method used for personnel dosimeters.

TLD is based on materials which (after exposure to ionizing radiation) emit light while they are heated. The impurities in the TL material give rise to localized energy levels within the forbidden energy band gap and that these are crucial to the TL process. As a means of detecting the presence of these defect levels, the sensitivity of TL is unrivalled. Townsend and Kelly [21] estimate that the technique is capable of detecting as few as 10^9 defects levels in a specimen. To put this number into perspective one should realize that detectable chemical `purity' in a sample is six orders of magnitude higher. The high sensitivity, allows the determination of very low radiation doses. On the other hand, it handicappes us in investigation into the relation between the luminescence and the defects involved in this process. The sensitivity of thermoluminescent material varies depending on the type of dosimeter.

TL is a luminescence phenomenon of an insulator or semiconductor which can be observed when the solid is thermally stimulated. TL should not be confused with the light spontaneously emitted from a substance when it is heated to incandescence. At higher temperatures (say in excess of 200°C) a solid emits (infra) red radiation of which the intensity increases with increasing temperature. This is thermal or black body radiation. TL, however, is the thermally stimulated emission of light following the previous absorption of energy from radiation. According to this phenomenon, the three essential ingredients necessary for the production of TL can be deduced. Firstly, the material must be an insulator or semiconductor–metals do not exhibit luminescent properties.

Secondly, the material must have at some time absorbed energy during exposure to ionizing radiation. Thirdly, the luminescence emission is triggered by heating the material [22]. A thermoluminescent material is a material that absorbs some energy which is stored during exposure to ionizing radiation. When the material is heated, the stored energy is released in the form of visible light as seen in Fig.2.1. In fact that TL does not refer to thermal *excitation*, but to *stimulation* of

luminescence in a sample which was excited in a different way. TL material can not emit light again by simply cooling the sample and reheating it another time. It should first be re-exposed to ionizing radiation before it produces light again. The storage capacity of a TL material makes it suitable for dosimetric applications.

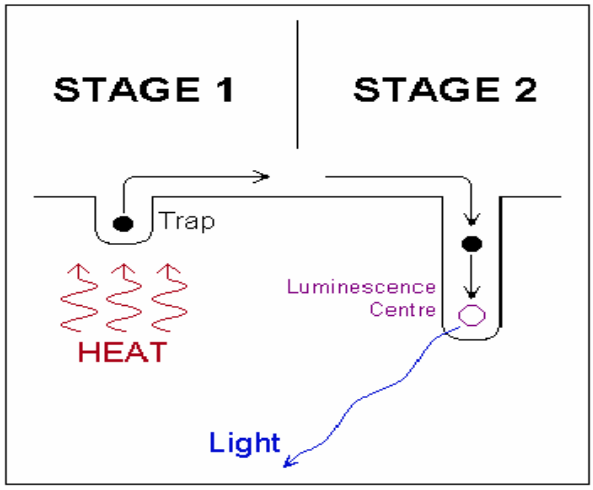

Figure 2.1 Phenomena of thermal excitation of luminescence

2.2. The One Trap–One Centre Model

The energy band theory of solids explains the observed TL properties. In an ideal semiconductor or insulator crystalline most of the electrons reside in the valence band. The next highest band that the electrons can occupy is the conduction band, separated from the valence band by the so-called forbidden band gap. The energy difference between the valence band and conduction band is E_g. However, whenever structural defects occur in a crystal, or if there are impurities within the lattice, there is a possibility for electrons to possess energies which are forbidden in the perfect crystal. In a simple TL model two levels are assumed, one situated below the bottom of the conduction band and the other situated above the top of the valence band (Fig. 2.2). The highest level indicated by T is situated above the equilibrium Fermi level (E_f) and thus empty in the equilibrium state, i.e. before the exposure to radiation and the creation of electrons and holes. It is therefore a potential electron trap. The other level (indicated by R) is a potential hole trap and can function as a recombination centre.

The absorption of radiant energy with $h\gamma > E_g$ results in ionisation of valence electrons, producing energetic electrons and holes which will, after thermalization, produce free electrons in the conduction band and free holes in the valence band (transition a). The free charge carriers recombine with each other or become trapped. In the case of direct recombination an amount of energy will be released which may excite a luminescent centre.

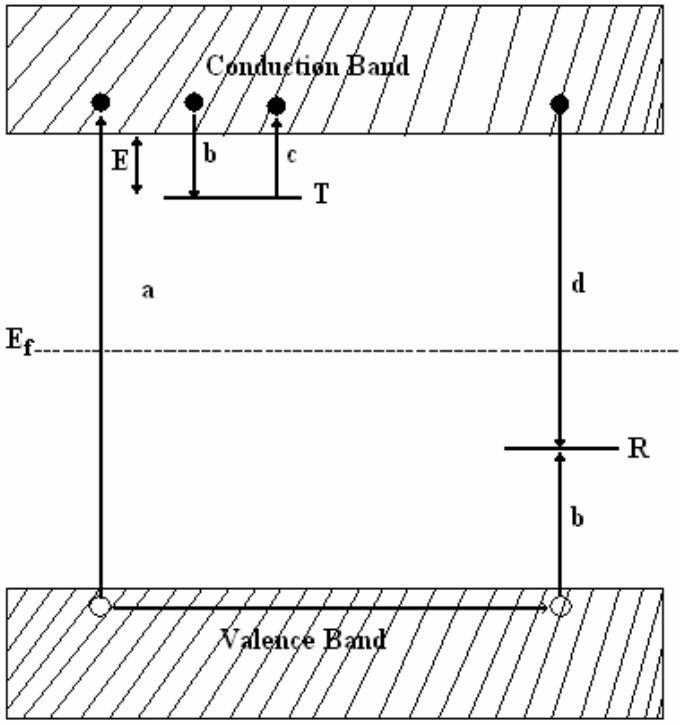

Figure 2.2 Energy band model showing the electronic transitions in a TL material according to a simple two-level model (a) generation of electrons and holes; (b) electron and hole trapping; (c) electron release due to thermal stimulation; (d) recombination. (•) shows electrons, (o) shows holes. Level T is an electron trap, level R is a recombination centre, E_f is Fermi level

The luminescent centre relaxes (returns to the ground state) under the emission of light. However, in semiconductors and insulators a certain percentage of the charge carriers are trapped: the electrons at T and the holes at R (transition b). The probability per unit time of release of an electron from the trap is assumed to be described by the Arrhenius equation,

$$p = s \exp\left\{-\frac{E}{kT}\right\} \tag{2.1}$$

where p is the probability per unit time, s is the frequency factor [18]. In the simple model s is constant; E is called the trap depth or activation energy, the energy needed to release an electron from the trap into the conduction band (see Fig.2.2).

The other symbols have their usual meaning: k is Boltzmann's constant=8.617×10^{-5} eV/K, and T is the absolute temperature. If the trap depth $E>>kT_0$, with T_0 the temperature at irradiation, trapped electrons will remain for a long period of time, until exposure to the radiation there will exist a substantial population of trapped electrons. There must be an equal population of trapped holes at level R, due to the free electrons and holes created and annihilated in pairs. Because the normal equilibrium Fermi level E_f is situated below level T and above level R, these populations of trapped electrons and holes represent a non-equilibrium state. The reaction path for return to equilibrium is always open, but because the perturbation from equilibrium (during exposure to ionising radiation) was performed at low temperature (compared to E/k), the relaxation rate as determined by Eq. 2.1 is slow. Thus, the non-equilibrium state is metastable and will exist for an indefinite period, governed by the rate parameters E and s.

The return to equilibrium can be speeded up by raising the temperature of the TL material above T_0. This will increase the probability of detrapping and the electrons will now be released from the trap into the conduction band. The charge carrier migrates through the conduction band of the crystal until it undergoes recombination at recombination centre R. In the simple model this recombination centre is a luminescent centre where the recombination of the electron and hole leaves the centre in one of the higher excited states. Return to the ground state is coupled with the emission of light quanta, i.e. TL. The intensity of TL $I(t)$ in photons per second at any time t during heating is proportional to the rate of recombination of holes and electrons at R. If m (m^{-3}) is the concentration of holes trapped at R the TL intensity can be written as

$$I(t) = -\frac{dm}{dt} \tag{2.2}$$

Here we assume that each recombination produces a photon and that all produced photons are detected. The rate of recombination will be proportional to the concentration of free electrons in the conduction band n_c and the concentration of holes m,

$$I(t) = -\frac{dm}{dt} = n_c m A \tag{2.3a}$$

with the constant A the recombination probability expressed in units of volume per unit time which is assumed to be independent of the temperature. The rate of change of the concentration of trapped electrons n is equal to the rate of thermal release minus the rate of retrapping,

$$-\frac{dn}{dt} = np - n_c(N-n)A_r \tag{2.3b}$$

with N the concentration of electron traps and A_r the probability of retrapping (m^3/s). Likewise the rate concentration of free electrons is equal to the rate of thermal release minus the rate of retrapping and the rate of recombination,

$$\frac{dn_c}{dt} = np - n_c(N-n)A_r - n_c m A \tag{2.3c}$$

Eqs.(2.3a)-(2.3c) described the charge carrier traffic in the case of release of a trapped electron from a single-electron trap and recombination in a single centre. For TL produced by the release of holes the rate equations are similar to Eqs.(2.3a)-(2.3c). These equations form the basis of many analyses of TL phenomena. There is no general analytical solution. To develop an analytical expression some simplifying assumptions must be made. An important assumption is at any time

$$\left|\frac{dn_c}{dt}\right| << \left|\frac{dn}{dt}\right|, \qquad \left|\frac{dn_c}{dt}\right| << \left|\frac{dm}{dt}\right| \tag{2.4}$$

This assumption is called by Chen and McKeever [18] the quasiequilibrium assumption since it requires that the free electron concentration in the conduction band is quasistationary. The trapped electrons and holes are produced in pairs during the irradiation. Charge neutrality dictates therefore

$$n_c + n = m \tag{2.5}$$

which for $n_c \approx 0$ means that $n \approx m$ and

$$I(t) = -\frac{dm}{dt} \approx -\frac{dn}{dt} \tag{2.6}$$

Since $dn_c/dt \approx 0$ one gets from (2.3a) and (2.3b):

$$I(t) = \frac{mAns \exp\left\{-\frac{E}{kT}\right\}}{(N-n)A_r + mA} \tag{2.7}$$

2.2.1. First-order kinetics

Even (2.7) cannot be solved analytically without additional simplifying assumptions. Randall and Wilkins [23,24] assumed negligible retrapping during the heating stage, i.e. they assumed $mA >> (N-n)A_r$. Under this assumption Eq.(2.7) can be written

$$I(t) = -\frac{dn}{dt} = sn \exp\left\{-\frac{E}{kT}\right\} \tag{2.8}$$

This differential equation describes the charge transport in the lattice as a first-order process and the glow peaks calculated from this equation are called first-order glow peaks. Solving the differential equation (2.8) yields

$$I(t) = -\frac{dn}{dt} = n_o s \exp\left\{-\frac{E}{kT}\right\} \exp\left\{-s\int_0^t \exp\left\{-\frac{E}{kT(t')}\right\} dt'\right\} \tag{2.9}$$

where n_0 is the total number of trapped electrons at time t=0. Usually the temperature is raised as a linear function of time according to

$$T(t) = T_o + \beta t \tag{2.10}$$

with β the constant heating rate and T_0 the temperature at t=0. This gives for the intensity as function of temperature

$$I(T) = -\frac{1}{\beta}\frac{dn}{dt} = n_o \frac{s}{\beta} \exp\left\{-\frac{E}{kT}\right\} \exp\left\{-\frac{s}{\beta}\int_{T_o}^{T} \exp\left\{-\frac{E}{kT'}\right\} dT'\right\} \tag{2.11}$$

This is the well-known Randall–Wilkins first-order expression of a single glow peak. The peak has a characteristic asymmetric shape being wider on the low temperature side than on the high temperature side. On the low temperature side, i.e. in the initial rise of the glow peak, the intensity is dominated by the first exponential (exp (-E/kT)). Thus, if I is plotted as function of 1/T, a straight line is expected in the

initial rise temperature range, with the slope of -E/k, from which the activation energy E is readily found.

The properties of the Randall–Wilkins equation are illustrated in Fig.2.3. In Fig.2.3 (a) it is shown how $I(T)$ varies if n_0 varies from n_0=0.25 m^{-3} till n_0=2 m^{-3} while E=1 eV, s=1.0×10^{12} s^{-1} and β=1 K/s are kept constant. It can be noted that the temperature at the peak maximum, T_m, stays fixed. This is a characteristic of all first-order TL curves. The condition for the maximum can be found by setting dI/dt=0 (or, somewhat easier from dln$I(T)$/dt=0). From this condition one gets

$$\frac{\beta E}{kT_m^2} = s \exp\left\{-\frac{E}{kT_m}\right\} \tag{2.12}$$

In this equation n_0 does not appear which shows that T_m does not depend on n_0. From Fig.2.3 (a) it can be further seen that not only the peak height at the maximum but each point of the curve is proportional to n_0. In the application in dosimetry n_0 is the parameter of paramount importance since this parameter is proportional to the absorbed dose. It is simple to see that the area under the glow peak is equal to n_0 since

$$\int_0^\infty I(t)dt = -\int_0^\infty \frac{dn}{dt}dt = -\int_{n_0}^{n_\infty} dn = n_0 - n_\infty \tag{2.13}$$

and n_∞ is zero for $t\to\infty$. In Fig.2.3 (b) the activation energy E has been varied from 0.8 to 1.2 eV. As E increases the peak shifts to higher temperatures with a decrease in the height and an increase in the width keeping the area (i.e. n_0) constant.

Similar changes can be noticed as s is varied (see Fig.2.3(c)) but now in the opposite way: as s increases the peak shifts to lower temperatures with an increase of the height and a decrease in width. In Fig.2.3 (d) the heating rate has been varied. As β increases the peak shifts to higher temperatures while the height decreases and the width increases just as in the case of decreasing s. This can be expected since s and β appear as a ratio s/β in Eq. (2.11). It is worthwhile to note that of the four parameters the activation energy E and the frequency factor s are the main physical parameters. They are called the trapping parameters and are fixed by the properties of the trapping centre. The other two parameters can be chosen by the experimenter by choosing a certain dose (n_0) and by read-out of the signal at a certain heating rate β. Investigation of a new TL material will therefore start with studying the glow peak behaviour under variation of the absorbed dose and the heating rate.

The evaluation of Eqn. (2.11) is hampered by the fact that the integral on the right-hand side is not elementary in the case of linear heating. Chen [25] has shown how the integral can be approximated by asymptotic series. In practical applications it is convenient to describe the glow peak in terms of parameters which are easy to derive experimentally, namely the intensity of peak at the maximum I_m and the temperature at the maximum T_m. Kitis et al. [26] have shown that Eqn. (2.11) can be quite accurately approximated by

$$I(T) = I_m \exp\left[1 + \frac{E}{kT}\frac{T-T_m}{T_m} - \frac{T^2}{T_m^2}\exp\left\{\frac{E}{kT}\frac{T-T_m}{T_m}\right\}(1-\Delta) - \Delta_m\right] \qquad (2.14)$$

with $\Delta=2kT/E$ and $\Delta_m=2kT_m/E$. Recently Pagonis et al. [27] have shown that a Weibull distribution function also accurately describes the first-order TL curve. These expressions may be convenient for peak fitting purposes.

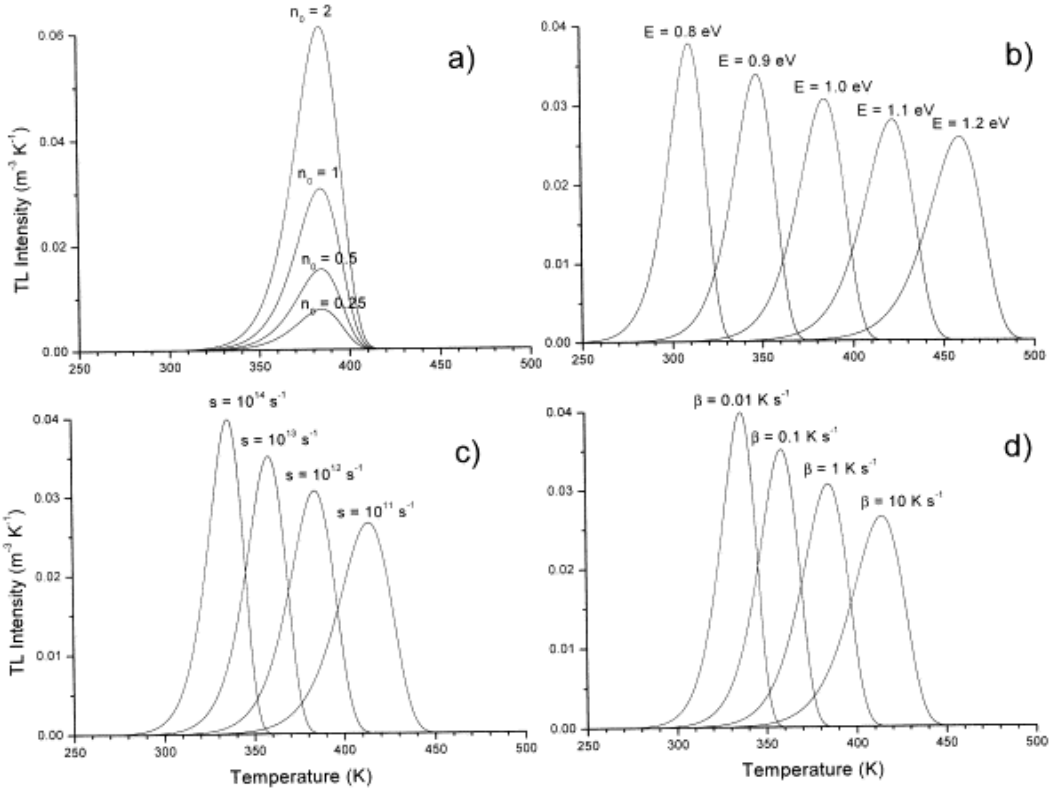

Figure 2.3 Properties of the R–W first-order TL equation, showing: (a) variation with n_0, the concentration of trapped charge carriers after irradiation; (b) the variation with E, the activation energy; (c) the variation with s, the escape frequency; (d) the variation with β, the heating rate. Parameter values: n_0=1 m^{-3}; E=1 eV; s=1×10^{12} s^{-1}, β=1 K/s of which one parameter is varied while the others are kept constant

2.2.2. Second-order kinetics

Garlick and Gibson [28] considered the possibility that retrapping dominates, i.e. $mA<<(N-n)A_r$. Further they assume that the trap is far from saturation, i.e. $N>>n$ and $n=m$. With these assumptions, Eqn.(2.7) becomes

$$I(t) = -\frac{dn}{dt} = s\frac{A}{NA_r}n^2 \exp\left\{-\frac{E}{kT}\right\} \tag{2.15}$$

We see that now dn/dt is proportional to n^2 which means a second-order reaction. With the additional assumption of equal probabilities of recombination and retrapping, $A=A_r$, integration of Eqn.(2.15) gives

$$I(T) = \frac{n_0^2}{N}\frac{s}{\beta}\exp\left\{-\frac{E}{kT}\right\}\left[1+\frac{n_0 s}{N\beta}\int_{T_0}^{T}\exp\left\{-\frac{E}{kT'}\right\}dT'\right]^{-2} \tag{2.16}$$

This is the Garlick–Gibson TL equation for second-order kinetics. The main feature of this curve is that it is nearly symmetric, with the high temperature half of the curve slightly broader than the low temperature half. This can be understood from the consideration of the fact that in a second-order reaction significant concentrations of released electrons are retrapped before they recombine, in this way giving rise to a delay in the luminescence emission and spreading out of the emission over a wider temperature range. The initial concentration n_0 appears here not merely as a multiplicative constant as in the first-order case, so that its variation at different dose levels change the shape of the whole curve. This is illustrated in Fig.2.4(a). It is seen that T_m decreases as n_0 increases. It can be derived [29] that the temperature shift can be approximated by

$$T_1 - T_2 \approx T_1 T_2 \frac{k}{E}\ln f \tag{2.17}$$

where T_1 is the temperature of maximum intensity at a certain dose and T_2 the temperature of maximum intensity at f times higher dose. With the parameter values of Fig.2.4 (a) the shift is 25 K. When E=1 eV, T_1=400 K and the absorbed dose is increased by a factor 1000, which is easy to realise experimentally, a temperature shift of 77 K can be expected. From Eqn.(2.17) it follows further that for a given increase of the dose the shallower the trap, i.e., the smaller E, the larger the peak shift. Fig.2.4 (b) illustrates the variation in size and position of a second-order peak as function of E, in Fig.2.4(c) s function of s/N, and in Fig.2.4 (d) as function of the

heating rate. The area under the curve is, as in the case of first-order kinetics, proportional to the initial concentration n_0 but the peak height is no longer directly proportional to the peak area, although the deviation is small.

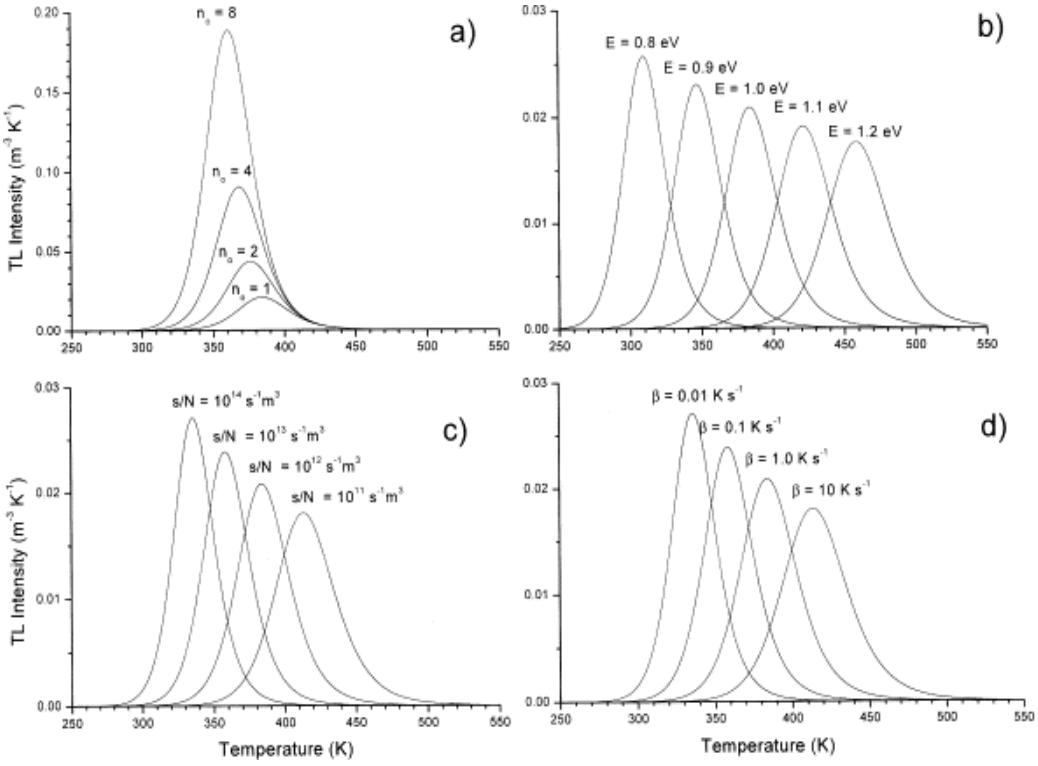

Figure 2.4 Properties of the Garlick–Gibson second-order TL equation, showing: (a) variation with n_0, the concentration of trapped charge carriers after irradiation; (b) the variation with E, the activation energy; (c) the variation with s/N; (d) the variation withβ, the heating rate. Parameter values: n_0=1 m^{-3}; E=1 eV; s/N=1×10^{12} s^{-1} m^3, β=1 K/s of which one parameter is varied while the others are kept constant

Note that, similarly to the first-order case, the term dominating the temperature dependence in the initial rise is exp(-E/kT). So the `initial rise method' for the determination of the trap depth can be applied here as well.

Also for second-order kinetics the glow peak shape, Eqn.(2.16) can be approximated with a function written in terms of maximum peak intensity I_m and the maximum peak temperature T_m [26]

$$I(T) = 4I_m \exp\left(\frac{E}{kT}\frac{T-T_m}{T_m}\right) \times \left[\frac{T^2}{T_m^2}(1-\Delta)\exp\left\{\frac{E}{kT}\frac{T-T_m}{T_m}\right\} + 1 + \Delta_m\right]^{-2} \qquad (2.18)$$

with Δ and Δ_m the same meaning as in Eqn.(2.14).

2.2.3. General-order kinetics

The first- and second-order forms of the TL equation have been derived with the use of specific, simplifying assumptions.

However, when these simplifying assumptions do not hold, the TL peak will fit neither first- nor the second-order kinetics. May and Partridge [30] used for this case an empirical expression for general-order TL kinetics, namely

$$I(t) = -\frac{dn}{dt} = n^b s' \exp\left\{-\frac{E}{kT}\right\} \tag{2.19}$$

where s' has the dimension of $m^{3(b\text{-}1)}$ s^{-1} and b is defined as the general-order parameter and is not necessarily 1 or 2. Integration of Eqn.(2.19) for $b \neq 1$ yields

$$I(T) = \frac{s''}{\beta} n_0 \exp\left\{-\frac{E}{kT}\right\}\left[1 + (b-1)\frac{s''}{\beta}\int_{T_0}^{T} \exp\left\{-\frac{E}{kT'}\right\} dT'\right]^{-b/(b-1)} \tag{2.20}$$

where now $s''=s' n_0^{b-1}$ with unit s^{-1}. Eqn.(2.20) includes the second-order case (b=2) and reduces to Eqn.(2.11) when $b \to 1$. It should be noted that according to Eqn.(2.19) the dimension of s' should be $m^{3(b\text{-}1)}$ s^{-1} that means that the dimension changes with the order b which makes it difficult to interpret physically. Still, the general-order case is useful since intermediate cases can be dealt with and it smoothly goes to first- and second-orders when $b \to 1$ and $b \to 2$, respectively (see Fig.2.5).

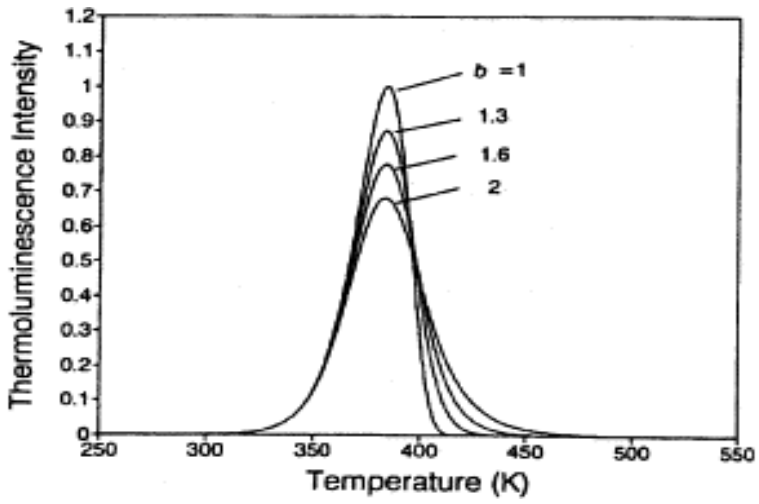

Figure 2.5 Comparison of first-order (b=1), second-order (b=2) and intermediate-order (b=1.3 and 1.6) TL peaks, with E=1 eV, $s=1\times10^{12}$ s^{-1}, $n_0=N$=1 m^{-3} and β=1 K/s (from [26])

2.2.4 Advanced models

The one trap–one centre model shows all the characteristics of the phenomenon TL and explains the behaviour of the glow peak shape under variation of the dose and heating rate. However, there is no existing TL material known that accurately is described by the simple model. This does not mean that the simple model has no meaning. On the contrary, it can help us in the interpretation of many features which can be considered as variations of the one trap–one centre model. There is no room to discuss all the advanced (more realistic) models in detail. The reader is referred to the text book of Chen and McKeever [18] for a deeper and quantitative treatment. Here, only some models are very briefly mentioned in order to get some idea about the complexity of the phenomenon in a real TL material.

In general, a real TL material will show more than one single electron trap. Not all the traps will be active in the temperature range in which the specimen is heated. A thermally disconnected trap is one which can be filled with electrons during irradiation but which has a trap depth which is much greater than the active trap such that when the specimen is heated only electrons trapped in the active trap (AT) and the shallow trap (ST) (see Fig.2.6(a)) are freed. Electrons trapped in the deeper levels are unaffected and thus this deep electron trap (indicted in Fig.2.6 (a) with DET) is said to be thermally disconnected. But its existence has a bearing on the trapping filling and eventually on the shape of the glow peak [31].

In Section 2.1 it was assumed that the trapped electrons are released during heating while the trapped holes are stable in the recombination centre. A description in which the holes are released and recombine at a centre where the electrons are stable during heating is mathematically identical. However, the situation will change if both electrons and holes are released from their traps at the same time at the same temperature interval and the holes are being thermally released from the same centres as are acting as recombination sites for the thermally released electrons and vice versa (see Fig.2.6 (b)). In this case Eqn.(2.2) is no longer valid. New differential equations should be drafted. Analysis of this complicated kinetic model reveals a TL glow curve which retains the simple Randall–Wilkins (Eqn.(2.11)) or Garlick–Gibson (Eqn.(2.16)) shape, depending upon the chosen values of the parameters. However, the E and s values used in Eqn.(2.11) and Eqn.(2.16) in order to obtain a fit on this complicated kinetic model need further interpretation.

Another process which might happen is a recombination without a transition of the electron into the conduction band (Fig.2.6(c)) Here the electron is thermally stimulated into an excited state from which a transition into the recombination centre is allowed. This means that the trap has to be in the proximity of a centre.

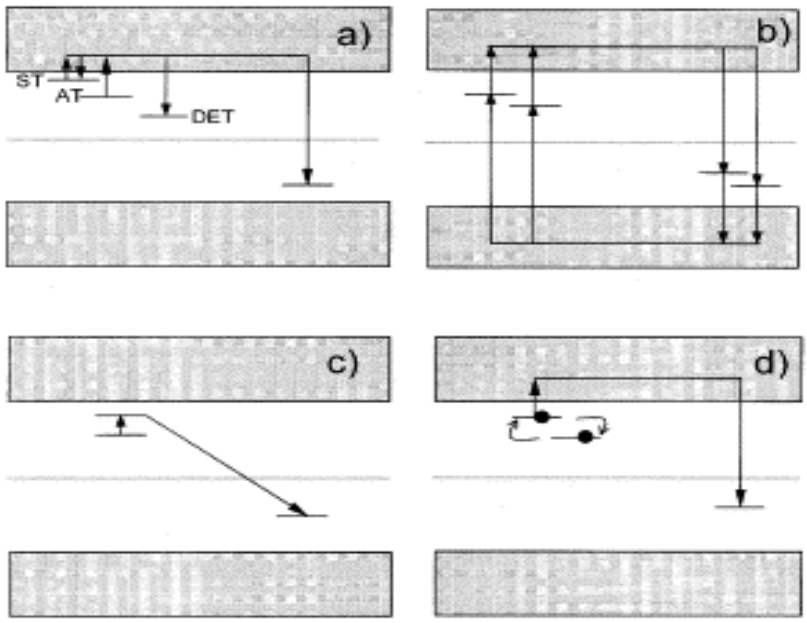

Figure 2.6 Advanced models describing the thermally stimulated release of trapped charged carriers including: (a) a shallow trap (ST), a deep electron trap (DET), and a active trap (AT); (b) two active traps and two recombination centres; (c) localised transitions; (d) defect interaction (trapping centre interacts with another defect)

The transition probability may strongly depend on the distance between the two centres. Under certain assumptions an expression for the TL intensity can be derived [31] which has the same form as Eqn.(2.11) but with *s* replaced by a quantity related to the probability for recombination. This means that these localised transitions are governed by first-order kinetics.

Finally, we will mention the possibility that the defect which has trapped the electron is not stable but is involved in a reaction with another defect (Fig.2.6 (d)). The result may be that at low temperature the trap depth is changing while the trapped electron concentration is stable. At higher temperatures electrons are involved in two processes: the escape to the conduction band and the defect reaction. Piters and Bos [32] have defect reactions incorporated into the rate equations and glow curves simulated. It appears that the simulated glow curves can be very well

fitted by Eqn.(2.11) It is clear that (again) the fitting parameters do not have the simple meaning of trap depth and escape frequency.

2.3. Trapping Parameter Determination Methods

The determination of trapping parameters from thermoluminescence glow curves has been a subject of interest for half a century. There are various methods for evaluating the trapping parameters from the glow curves [23-24, 31, 33-37].

When one glow peak is highly isolated from the others, the experimental methods such as initial rise, variable heating rates, isothermally decay, and peak shape methods are suitable methods to determine these parameters. However in most materials, the glow curve consists of several peaks as in the APSQ. In case of overlapping peaks there are essentially two ways to obtain these parameters, the first one is the partial thermal cleaning method and the second one is the computer glow curve deconvolution program. In most cases, the partial thermal cleaning method can not be used to completely isolate the peak of interest without any perturbation on it. Therefore, the computer glow curve deconvolution program has become very popular method to evaluate trapping parameters from TL glow curves in recent years [38].

2.3.1 Peak shape method

Evaluation of E from the shape of the peak utilising parameters such as T_m, full width at half-maximum $\omega=T_2-T_1$, half width on the high temperature side of the maximum $\delta=T_2-T_m$, half width on the low-temperature side of the maximum $\tau=T_m-T_1$, and $\mu_g=\delta/\omega$ called the shape parameter.

The order of kinetics b can be estimated by means of shape parameters. Chen [33] found that μ_g is not sensitive to changes in E and s, but it changes with the order of kinetics b. It has been shown that the ranges of μ_g varies from 0.42 for b=1 to 0.52 for b=2 in case of linear heating.

The first peak shape method was developed by Grossweiner [34]; later Chen [33] modified Halperin and Braner's equations [35] for calculating E values;

$$E_\tau = \left[1.51 + 3(\mu_g - 0.42)\right]\frac{kT_m^2}{\tau} - \left[1.58 + 4.2(\mu_g - 0.42)\right]2kT_m$$
$$E_\delta = \left[0.976 + 7.3(\mu_g - 0.42)\right]\frac{kT_m^2}{\delta} \tag{2.21}$$
$$E_\omega = \left[2.52 + 10.2(\mu_g - 0.42)\right]\frac{kT_m^2}{\omega} - 2kT_m$$

After determination of the activation energy and the order of kinetics, using the following expressions the frequency factor *s*, it must be noted that this parameter called as pre-exponential factor in the general order kinetic, can be estimated for first and general order kinetics respectively.

$$s = \frac{\beta E}{kT_m^2}\ \exp\left[\frac{E}{kT_m}\right]$$
$$s = \frac{\beta E}{kT_m^2}\left[\exp(-\frac{E}{kT_m})(1 + (b-1)\frac{2kT_m}{E})\right]^{\frac{b}{b-1}} \tag{2.22}$$

2.3.2 Isothermal decay method

The isothermal decay is quite a different method of analysis of the trapping parameters in which the TL sample temperature is kept constant and the light emission can be recorded as a function of time. Generally, in the isothermal decay method, the following equation is solved for constant *T* for the first order kinetics

$$I(T) = -c\frac{dn}{dt} = c\frac{n_0}{\tau}\exp(-\frac{t}{\tau}) \tag{2.23}$$

where n_0 is the initial value of *n* and $\tau = s^{-1}\exp(\frac{E}{kT})$.

The above equation shows that at a constant temperature *T*, the light emission will decay exponentially with time *t* and a plot of *ln(I)* against *t* will give a straight line with a slope $m = s\exp(-\frac{E}{kT})$. In order to find *E* and *s*, the experiments are carried out at two different constant temperatures T_1 and T_2, resulting in two different slopes m_1 and m_2. Thus the activation energy can be determined by using the following equation

$$E = \frac{k}{(\frac{1}{T_2} - \frac{1}{T_1})} \ln(\frac{m_1}{m_2}) \qquad (2.24)$$

The isothermal decay method is not applicable to higher order kinetics. In 1979; a method has been proposed by Kathuria and Sunta [39] to calculate the order of kinetics from the isothermal decay of thermoluminescence. According to this method; if the decaying intensity from the sample is held at a constant temperature, the plot of $I^{(\frac{1}{b}-1)}$ versus t gives a straight line, when the proper value of b is chosen. Therefore, various b values are tried and the correct one is that giving a straight line.

2.3.3 CGCD method

Computer Glow Curve Deconvolution (CGCD) is one of the most important method to determine trapping parameters from TL glow curves. This method has the advantage over experimental methods in that they can be used in largely overlapping-peak glow curves without resorting to heat treatment

In this study, a CGCD program was used to analyse the glow curve of APSQ. The program was developed at the Reactor Institute at Delft, The Netherlands [40]. This program is capable of simultaneously deconvoluting as many as nine glow peaks from glow curve. Two different models were used in the computer program. In the first model, the glow curve is approximated from first order TL kinetic by the expression,

$$I(T) = n_0 s \quad \exp(-\frac{E}{kT}) \exp\left[(-\frac{s}{\beta} \frac{kT^2}{E} \exp(-\frac{E}{kT}) * (0.9920 - 1.620 \frac{kT}{E_a}) \right] \qquad (2.25)$$

In the second model the glow curve is approximated with general order TL kinetics by using the expression,

$$I(T) = n_0 s \quad \exp(-\frac{E}{kT}) \left[1 + (-\frac{(b-1)s}{\beta} \frac{kT^2}{E} \exp(-\frac{E}{kT}) * (0.9920 - 1.620 \frac{kT}{E_a}) \right]^{\frac{b}{b-1}} \qquad (2.26)$$

where n_0 (m^{-3}) is the concentration of trapped electrons at t=0, s (s^{-1}) is the frequency factor for first-order and the pre-exponential factor for the general-order, E (eV) the activation energy, T (K) the absolute temperature, k (eVK^{-1}) Boltzmann's constant, β ($^0Cs^{-1}$) heating rate and b the kinetic order.

The summation of overall peaks and background contribution can lead to composite glow curve formula as shown below

$$I(T) = \sum_{i=1}^{n} I_i(T) + a + b\exp(T) \tag{2.27}$$

where *I(T)* is the fitted total glow curve, *a* allows for the electronic noise contribution to the planchet and dosimeters infrared contribution to the background.

Starting from the above equation (2.27), the least square minimisation procedure and also FOM (Figure of Merit) was used to judge the fitting results as to whether they are good or not. i.e.

$$FOM = \sum_{i=1}^{n} \frac{\left|N_i(T) - I(T)\right|}{A} = \sum_{i=1}^{n} \frac{\left|\Delta N_i\right|}{A} \tag{2.28}$$

where $N_i(T)$ is the i-th experimental points (total n=200 data points), *I(T)* is the i-th fitted points, and *A* is the integrated area of the fitted glow curve.

From many experiences [17,41], it can be said that if the values of the FOM are between 0.0% and 2.5% the fit is good, 2.5 % and 3.5% the fit is fair, and > 3.5% it is bad fit.

To have a graphic representation of the agreement between the experimental and fitted glow curves, the computer program also plots the function,

$$X(T) = \frac{N_i(T) - I_i(T)}{\sqrt{I_i(T)}} \tag{2.29}$$

which is a normal variable with an expected value 0 and σ=1 where $\sigma^2(T)=I_i(T)$.

2.3.4. Initial rise method

The simplest, and most generally applicable method for evaluating the activation energy *E* of a single TL peak is the initial rise method. The basic premise upon which this method is based is that at the low temperature end of the peak,all the relevant occupancies of the states, the trap, the recombination center and, in some cases, other interactive states can be considered as being approximately constant.

The rise of the measured intensity as a function of temperature in this region is, therefore, very close to exponential, thus

$$I(T) = C\exp(-E/kT) \tag{2.30}$$

where the constant C includes all the dependencies on the other parameters and occupancies, E is the activation energy (eV), k is the Boltzmann`s constant (eV/K^{-1}) and T is the temperature (K).

Plotting ln(I) against $1/T$ a linear plot is obtained with slope equal to $-E/k$. Hence it is possible to evaluate E without any knowledge of the frequency factor s by means of equation

$$E = -kd(\ln(I))/d(1/T) \tag{2.31}$$

Once the value of E was determined, the frequency factor (s) was obtained from the equation

$$\frac{\beta E}{kT_m} = s\exp(-\frac{E}{kT}) \tag{2.32}$$

where T_m is the temperature at the maximum intensity. This method can only be used when the glow peak is well defined and clearly seperated from the other peaks.

2.3.5. Heating rate method

Another important method is various heating rates for the determination of activation energies. If a sample is heated at two different linear heating rates β_1 and β_2 the peak temperatures will be different. Equation (2.32) can therefore, be written for each heating rate and dividing the equation for β_1 (and T_{m1}) by the equation for β_2 (and T_{m2}) and rearranging, one gets an explicit equation for the calculation of E

$$E = k\frac{T_{m1}T_{m2}}{T_{m1}-T_{m2}}\ln[(\frac{\beta_1}{\beta_2})(\frac{T_{m2}}{T_{m1}})^2] \tag{2.33}$$

The major advantage of the heating rate method is that it only requires data to be taken at a peak maximum (T_m, I_m) which, in case of a large peak surrounded by smaller satellites, can be reasonably accurately determined from the glow curve. Furthermore the calculation of E is not affected by problems due to thermal quenching, as with the initial rise method.

When various heating rates for the first-order kinetics are used, the following expression is obtained:

$$\ln(\frac{T_m^{\ 2}}{\beta}) = (\frac{E}{k})(\frac{1}{Tm}) + cons\tan t \qquad (2.34)$$

A plot of ln (T_m^2/β) versus ($1/ T_m$) should yield a straight line with a slope E/k, and then E is found. Additionally, extrapolating to $1/T_m = 0$, a value for $ln(sk/E)$ is obtained from which s can be calculated by inserting the value of E/k found from the slope.

These methods of various heating rates are applicable for general-order kinetics which includes the second-order case. For the general order case, one can plot $ln\left[I_m^{\ b-1}(T_m^{\ 2}/\beta)^b\right]$ versus $1/T_m$, whose slope is equal to E/k.

CHAPTER 3

EXPERIMENTAL PROCEDURE

The material, equipments and experimental procedures utilized in this work are described below.

3.1. Materials

The sample used in this study were CaF_2:Mn (TLD-400) crystal chips (3.2mm x 3.2mm x 0.89mm) which were obtained from Harshaw Chemical Company, Ohio, USA.

3.2. Equipments

3.2.1. Radiation source and irradiation procedure

The samples were annealed at 400±1^{0}C for 30 min through the experiments to erase any residual information before the subsequent irradiation and then cooled in air at ≈75 °C min^{-1} to room temperature. All annealing treatments were applied to the samples with a specially designed microprocessor-controlled electrical oven, which is able to control the temperature to within ±1 °C. All irradiations were performed immediately after the standart annealing at room temperature with β-rays from a ^{90}Sr-^{90}Y source (≈ 0,015 Gy/s). The activity of β-source is about 100 mCi. It is calibrated by manufacturer on March, 10, 1994. The recommended working life-time is about 15 years. Stronium-90 emits high energy beta particles from their daughter products (^{90}Sr β-0.546 MeV together with ^{90}Y β-2.27 MeV). Beta radiation is absorbed by air, so its intensity declines with distance much more rapidly than inverse square law calculations would indicate. The maximum range of Y-90 beta particles in air is approximately 9 meter. The irradiation equipment is an additional part of the 9010

Optical Dating System which is purchased from Little More Scientific Engineering, UK [42] the samples were irradiated to various dose levels between ≈0.015 and ≈110 Gy during the variable dose method. The irradiated samples were read out in an N_2 atmosphere with a Harshaw QS 3500 manual type reader which is having an S-11 response photomultiplier tube. The reader is interfaced to a PC where the TL signals were studied and analyzed. A standard clean glass filter was always installed in the reader between sample and photomultiplier tube. This filter allows the light whose wavelength is between ≈250 nm and ≈1000 nm to pass through the filter and thereby eliminates unwanted infrared light emitted from heater. Glow curves were measured using a platinum planchet at a linear heating rate of 1 °C s^{-1}. The time duration between irradiation and the TL reading was always kept constant at about 1 min. For the variable heating rate method, heating rates were varied from 1°C s^{-1} to 20 °C s^{-1}. At each experimental measurement, four chips were read out. Each chip was read out twice and the second readout is considered to be the background of the reader plus chip; this was subtracted from the first one and all of the analyses have been carried out after the subtraction [58].

3.2.2. TL analyzer and TL measurements

The glow curve measurements for CaF_2:Mn crystals were made using a Harshaw TLD System 3500 Manual TL Reader [22]. It economically provides high reliability. The technical architecture of the system includes both the Reader and a DOS-based IBM-compatible computer connected through a standard RS-232 serial communication port to control the 3500 Reader. The basic block diagram of reader is shown in figure 3.1. All functions are divided between the reader and the specialized TLDShell software that runs on the PC. All data storage, instrument control, and operator inputs are performed on the PC. Signal acquisition and conditioning are performed in the reader. In this way, each glow curve can be analyzed using a best-fit computer program based on a Marquardt algorithm minimisation procedure, associated to first-order and general-order kinetic expressions. The program resolves the individual peaks present in the curve, giving the best values for the different peak parameters.The instrument includes a sample change drawer for inserting and removing the TLD elements. The reader uses contact heating with a closed loop feedback system that

produces adjustable linearly ramped temperatures from 1 ^{o}C to 50 ^{o}C per second accurate to within ± 1 ^{o}C to 600 ^{o}C in the standard reader.

The Time Temperature Profile (TTP) is user defined in three segments: Preheat, Acquire, and Anneal, each with independent times (Pre-read anneal: adjustable 0 to 1000 sec, Linear ramp: adjustable from 1 ^{o}C to 50 ^{o}C per second, Post-read anneal: 0 to 1000 sec) and temperature (Pre-read anneal: room temperature to 200 ^{o}C, Post-read anneal: up to 400 ^{o}C). The typical time temperature profile is shown in figure 3.2. To improve the accuracy of low-exposure readings and to extend planchet life, the 3500 provides for nitrogen to flow around the planchet. By eliminating oxygen in the planchet area, the nitrogen flow eliminates the unwanted oxygen-induced TL signal. Nitrogen is also routed through the photo-multiplier tube (PMT) chamber to eliminate moisture caused by condensation. Glow curves were measured using a platinum planchet at a linear heating rate of 1 ^{o}C/s. The time duration between irradiation and necessary TL operation was always kept constant at about 1 min, except for the storage time experiment. For the variable heating rate method heating rates were varied from 1 to 20 ^{o}C/s. At each heating rate four chips were read out. Each chip was read out twice and the second readout is considered to be background of the reader plus chip and was subtracted from the first one and all of the analyses have been carried out after subtraction operations.

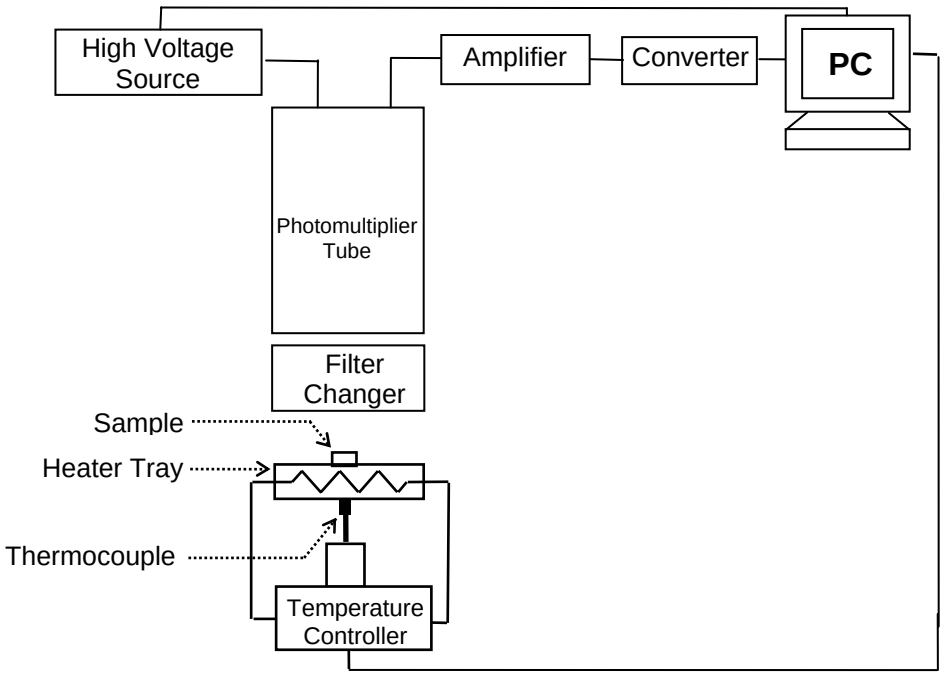

Figure 3.1 Basic block diagram of TL reader

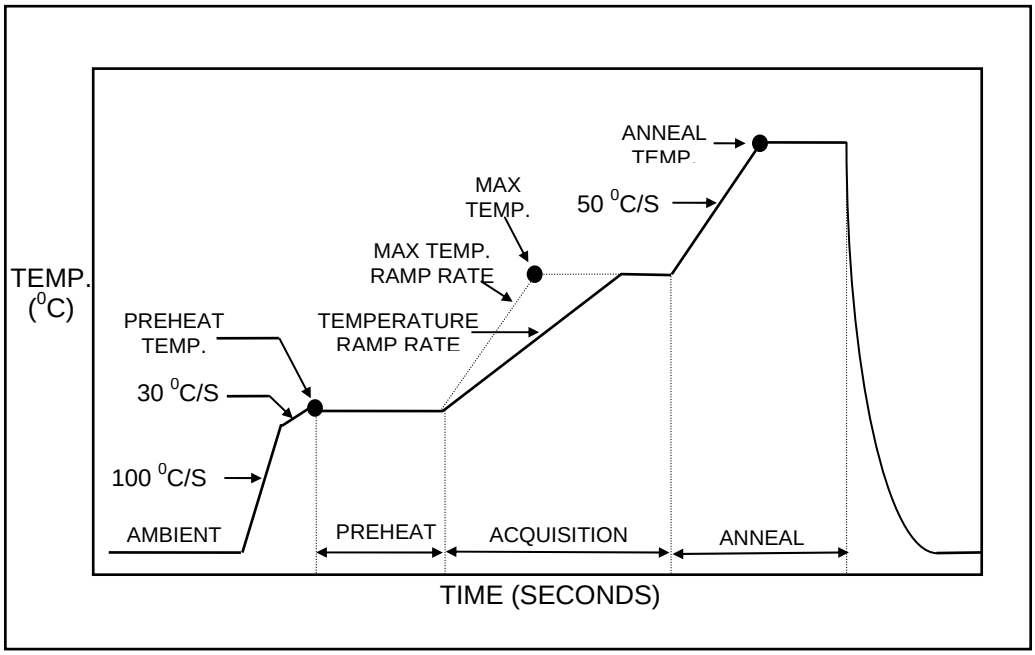

Figure 3.2 Typical time temperature profile (TTP)

3.3. Experimental Procedure for CaF_2:Mn

The sample was first heated up to 400 ºC to erase any residual information before the subsequent irradiation and then quickly cooled in air to room temperature. The sample was irradiated at room temperature with beta rays from a calibrated ^{90}Sr-^{90}Y source. The irradiated sample was read out in N_2 atmosphere with a Harshaw QS 3500 manual type reader that is interfaced to a PC where the TL signals were studied and analyzed. Glow curves were measured using a platinum planchet at a linear heating rate of 1 ºC/s. In a contact heating, the temperature control is achieved with the temperature of the heating element (planched) and therefore a thermal lag exists between samples and heater at high heating rate (> 2 ºC/s). A standart clean glass filter was always installed in the resder between samole and photomultiplier tube. This filter allows the light whose wavelength between ≈ 250 nm and ≈ 1000 nm to pass through it and thereupon eliminates unwanted infrared lights that are emitted from heater. The time duration between irradiation and TL reading was always kept constant at about 1 min. For the VHR method, the heating rates were varied from 1 to 20 ºC/s. At each experimental measurement, the sample

was read out and read out twice. The second readout is considered to be the background of the reader plus sample; this was subtracted from the first one and all of the analyses have been carried out after the subtraction.

CHAPTER 4

EXPERİMENTAL RESULTS

4.1. Results and Discussion

4.1.1. Annealing procedure of CaF_2:Mn

Before the investigation of TL properties of Mn-doped CaF_2, an annealing procedure was usually utilized to improve the performance of TL material before the irradiation, because; it is known that the heat-treatment before the irradiation is generally reestablished the defect equilibrium that exists in the material and the heating can also empty the deep traps to avoid its influence on the TL sensitivity of a given peak since they can act as competitors. Therefore, one of the first problems investigated in the given study is the annealing procedure to be used in order to eliminate the effects of the previous irradiations. In order to assess the reproducibility of the dose measurements attainable using CaF_2:Mn, the TL stability after repeated cycles of the both oven and readout annealing procedures was tested at different dose levels (0.45 Gy, 4.5 Gy and 45 Gy) and the comparison of TL sensitivity of TL dosimeters after oven and readout anneal was performed. The intensity is obtained by the integral of the peak area of the dosimetric glow peak at 298 ^{o}C. In the readout annealing procedures, firstly, some samples after their background reading were irradiated to a test dose ≈0.45 Gy (or 4.5, or 45 Gy). The samples were subsequently readout up to 400 ^{o}C with a linear heating rate of 1 ^{o}C/s, and their glow curves were recorded. After this readout the samples were irradiated again at the same test dose and then readout. The glow curve shapes and intensities were seen to be identical in all cases after the irradiation at ≈0.45 Gy. The results showed that the readout annealing procedures show a very good stability within less than 3% based on standard deviation over more than 10 repeated cycles for the dose levels below ≈0.5 Gy. However, for the dose levels exceeding ≈0.5 Gy, it was found that readout

annealing is insufficient to completely empty the deep traps in CaF_2:Mn and restore the original TL sensitivity of the TL dosimeters. As seen from the Fig.4.1, when the dose levels exceed ≈0.5 Gy, the intensity of dosimetric peak was increased ≈15-20% after ten repeated cycles of irradiation-readout annealing and, therefore, it was decided that an oven annealing is necessary to get a stable TL response and the lowest background. Therefore, the oven annealing procedures were carried out at 400 and 500 ^{o}C for 30 min and then the sample was rapidly cooled to room temperature after each heat treatment. The obtained results confirmed that when the samples are annealed in an oven at 500 ^{o}C for 15 min after irradiation with low or high doses, the intensity of dosimetric glow peak is continuously decreased with increasing experimental cycles. On the other hand, an oven annealing treatment at 400 ^{o}C for 30 min was found to be sufficient to erase TL signal completely and restore the original TL sensitivity of the TL dosimeters (Fig.4.1). As a result, it can be mentioned that during routine applications of TL detectors for dose levels less than ≈1 Gy, a readout annealing up to 400 ^{o}C appeared to be a convenient annealing procedure (Fig.4.1). Moreover, when the dose levels increased above ≈1 Gy (i.e for 4.5 or 45 Gy), it was observed that the readout annealing is not sufficient to erase TL signal completely. Consequently, if the previous history of the material is unknown, it is advantageous to anneal the sample at 400 ^{o}C for 30 min before putting it to any dosimetric use.

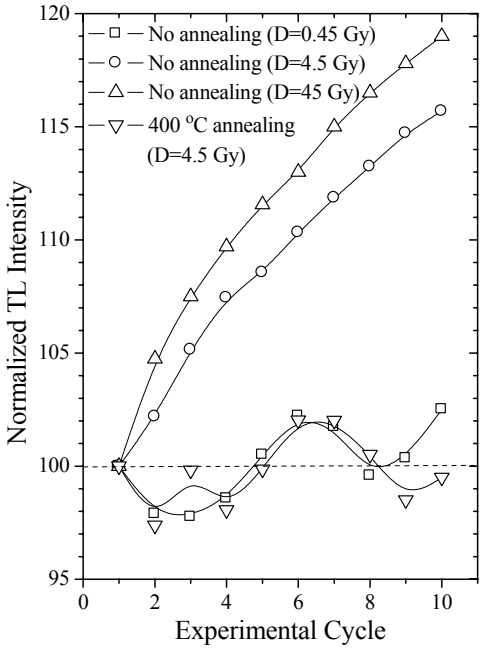

Figure 4.1 Reproducibility of deconvoluted area of dosimetric peak of Mn-doped CaF_2 through ten repeated cycles of irradiation-readout annealing

4.1.2. The glow curve analysis of CaF_2:Mn

Previously published studies have shown that the determination of E_a and s mainly depends on the prior knowledge of kinetic order (b) and the exact number of glow peaks in the glow curve [29, 43-46]. The investigations were based on the principle of different characteristic response patterns of glow peaks during irradiation. In most situations, the glow peaks grow linearly at low-level exposure. No significant discrimination in the shapes of overlapped peaks can be observed at this stage. As the exposure level increases, the growth of TL peaks would behave in different patterns. Some are still linear while others are supralinear or sublinear. Therefore, the highly overlapped glow peaks become distinguishable through a series of high-level irradiations. In TL theory [2, 16-19], the peak temperatures of glow peaks are expected to change only with heating rate for b=1. Hence, for a constant heating rate (β), the peak temperature should not be affected by other experimental parameters and should be fairly constant within the limit of experimental uncertainties.

However, for $b \neq 1$ and below the trap saturation points {n_o (concentration of trapped electrons) < N_t (concentration of traps)}, it is generally received that the peak temperatures are shifted to the lower-temperature side with increasing dose levels. Therefore, to form an opinion about the number of glow peaks and b of all individual glow peaks in the glow curve structure of CaF_2:Mn, the AD method was first utilized in the current study. Some of the selected glow curves after different dose levels are shown in Fig.4.2. The experimental observations have clearly shown that there were no significant changes in the peak temperature of glow peak of CaF_2:Mn with increasing dose level (Fig.4.2). The positions of peak temperature of this peak are within the experimental error ±4 ^oC for all the doses (Fig.4.3). This result indicates that the main glow peak or at least all of the individual glow peaks in the dosimetric glow peak of CaF_2:Mn should have first-order kinetics. On the other hand, the slight variations in the shape of glow peak with increasing dose levels are indicated that this peak no longer retains the original single pattern. This observation reveals the fact that main glow peak consists of more than one glow peak.

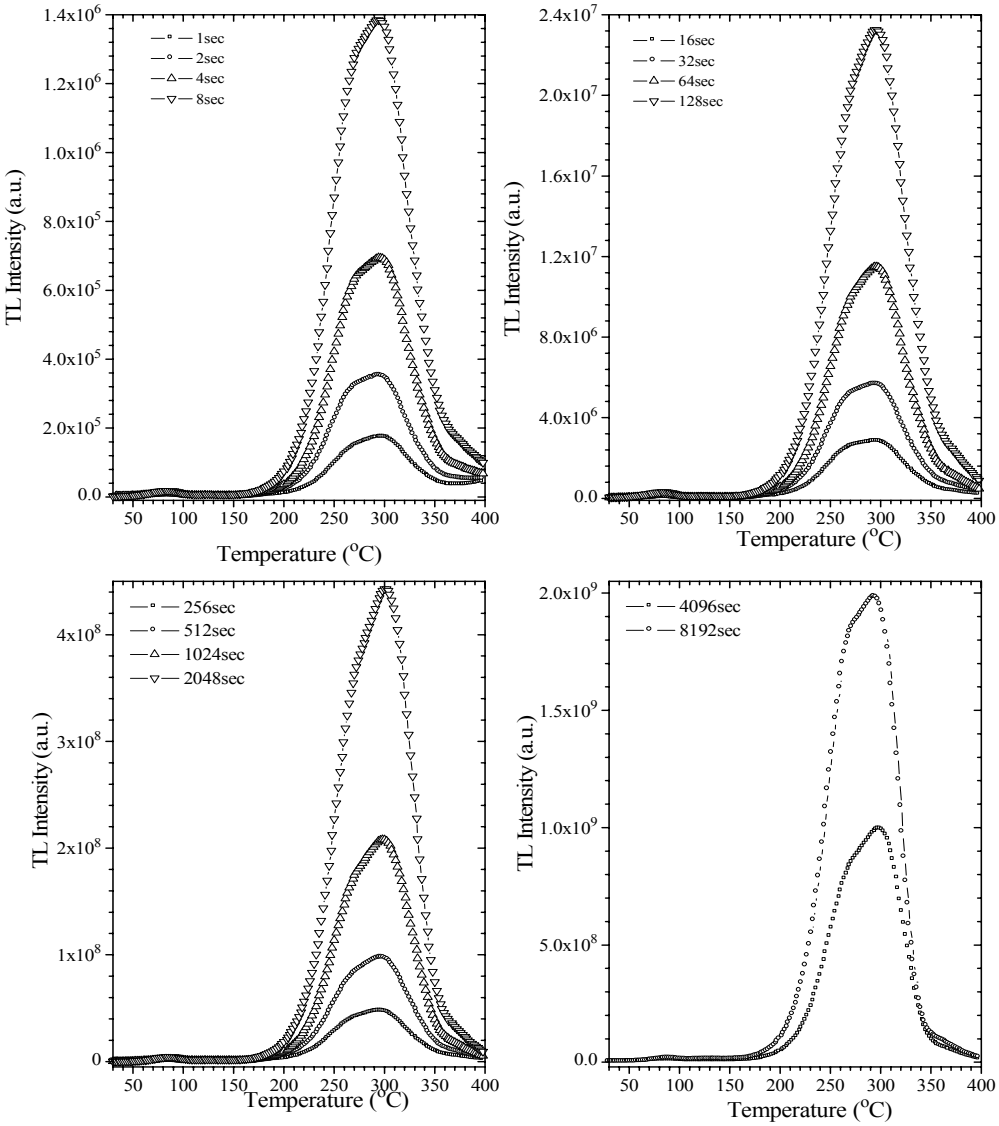

Figure 4.2 The glow curve of CaF_2:Mn measured after various radiation doses (β=1 $^{o}C\ s^{-1}$)

The recorded glow curves after the AD experiment were also used to test the possible number of glow peaks in the glow curve of CaF_2:Mn and their kinetic parameters by the PS method. This method is based on the shape and full width at half maximum (FWHM=T_2-T_1) of a single glow peak and the values of E_a were determined by the modified PS method of Chen [47]. According to this method, the b of a single peak is easily obtained by means of the geometric factor $\{\mu_g=(T_2-T_m)/(T_2-T_1)\}$ and μ_g changes with the order of kinetics b from ≈0.42 to ≈0.52, where these two limits correspond to first- and second-order kinetics, respectively.

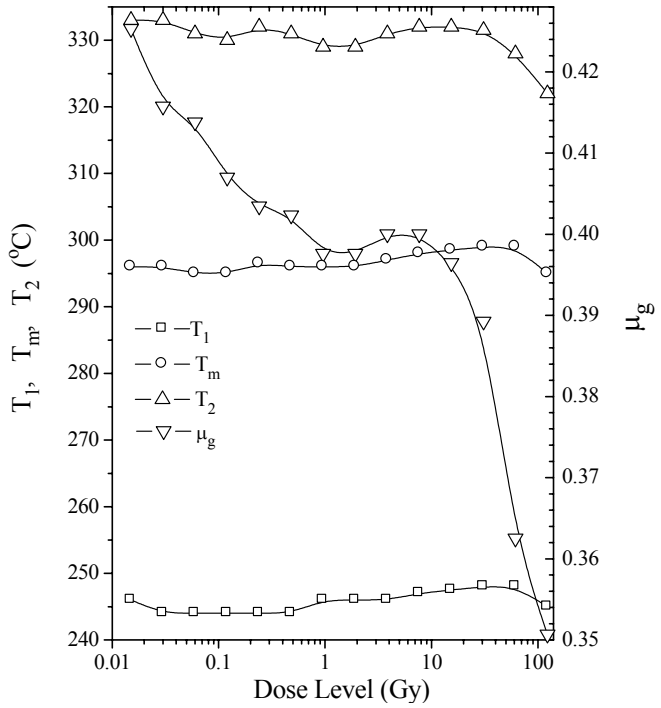

Figure 4.3 The peak temperature T_m, low half-maximum temperature T_1, high half-maximum temperature T_2, and geometric factor μ_g of glow peak of CaF_2:Mn as a function of exposed dose level

The shift in the low half-maximum temperature T_1, high half maximum temperature T_2 together with peak temperature T_m, and the variation in μ_g with exposed dose levels are also seen in Fig.4.3. When the dosimetric peak was considered to be a single peak, it was observed that μ_g is slightly greater than 0.42 for $D \approx 0.015$ Gy but quickly decreases from 0.425 to 0.40 between 0.015 and 1 Gy and then it follows a slight flat region between ≈1 and ≈10 Gy. If the dose level is increased above 10 Gy, μ_g starts decreasing again with increasing dose level and reaches ≈0.35 at around D=110 Gy, which corresponds to a kinetic order smaller than first-order. The occurrence of $b<1$ is physically impossible and meaningless. The variation of the shape of the dosimetric peak as a function of D indicates that this peak should have several overlapping glow peaks that have first- and/or general-order kinetics. The plots of calculated activation energies by the PS method are shown in Fig.4.4. Note that the dosimetric peak is assumed to have one component during the calculation of E_a by the PS method. The trend of E_a calculated by the PS method is fairly similar to the trend of μ_g after different dose levels. As seen from this figure, when the dose level is increased, the activation energies determined from the three shape parameters of the glow peak show slight decrease between 0.015 and 1 Gy. After slight smooth regions between ≈1 and ≈10 Gy, they quickly start to

decrease with increasing dose levels up to the applied maximum dose (D≈110 Gy) in the present study. This result again indicates that the dosimetric peak of this material is not a single peak and it is a superposition of many components.

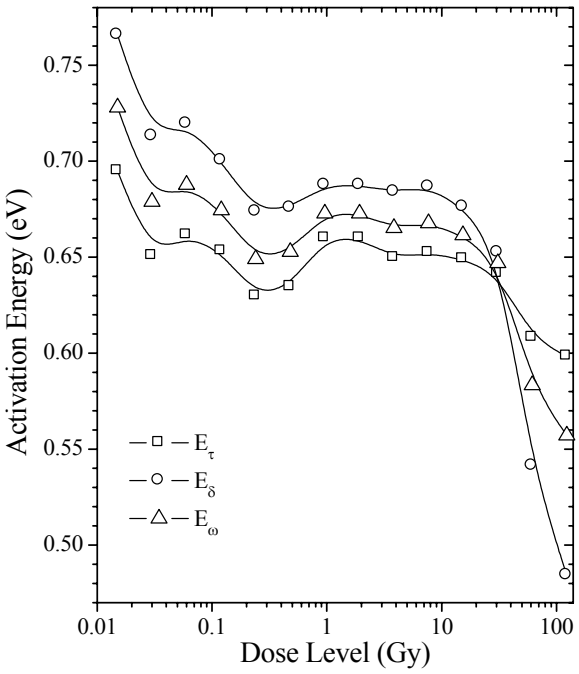

Figure 4.4 The activation energy E_a of the dosimetric glow peak of CaF_2:Mn determined by PS method as a function of dose levels (β = 1°C s^{-1})

4.1.3. Determination of number and position of glow peaks

In an attempt to better find the number of peaks, peak temperatures and their related kinetic parameters, the method of RIR was also applied to the TL glow curves of CaF_2:Mn in the temperature ranges from 200 ^oC to 380 ^oC. A strong overlapping of TL peaks makes this method the most suitable procedure for the determination of number and position of glow peaks. A plot of T_m against T_{stop} shows a stepwise curve after T_m–T_{stop} experiment and each flat region indicates the approximate position of an individual peak. A rise of T_m at the end of the flat region is an indication that the TL kinetics have an order higher than 1. Peaks with first-order TL kinetics show a sharp rise to the next flat region. However, in the case of highly overlapping glow peaks, the sharp rise can be slightly smoothened out. The process is repeated several times with the same annealed/irradiated sample at some different T_{stop} values, and two measurements were taken within each 10 ^oC region in this study. The heating rate used was 1 $^oCs^{-1}$ and the exposed dose level was always set to 4.5 Gy. Some of

the selected glow curves after T_m–T_{stop} procedure are shown in Fig.4.5. As seen from this figure, the T_m of the dosimetric glow peak is continuously shifted to the high temperature region with increasing T_{stop}.

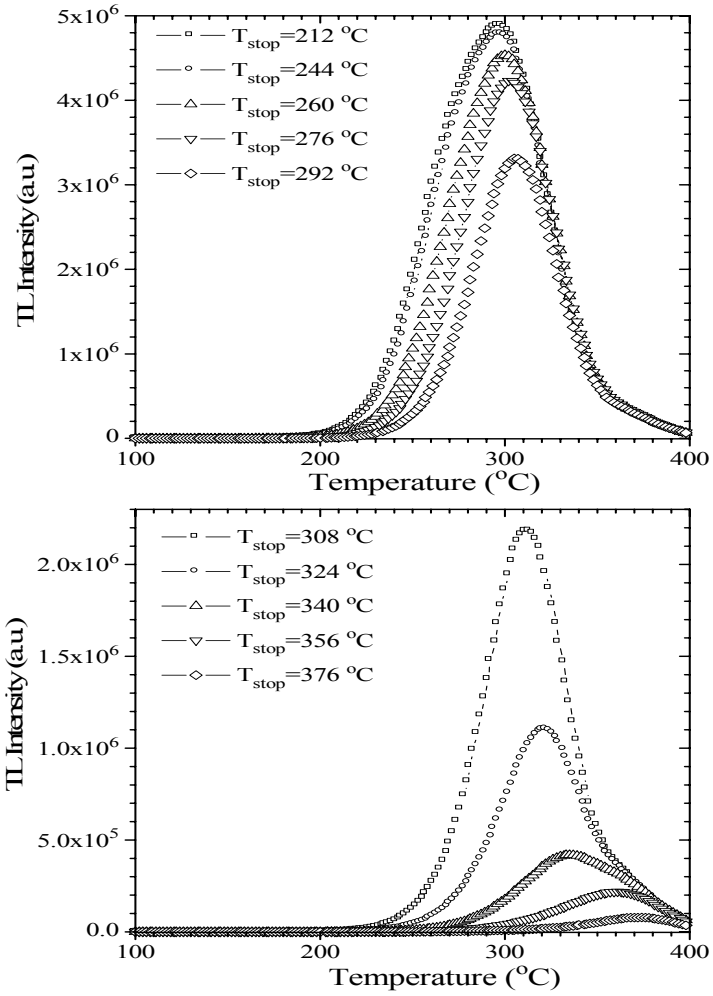

Figure 4.5 Some of the selected glow curves of CaF_2:Mn after different T_{stop} temperatures at a heating rate β = 1 °C s^{-1}. The exposed dose levels are always adjusted to ≈0.45 Gy

A plot of the I_m–T_{stop}, T_m–T_{stop}, T_1–T_{stop} and T_2–T_{stop} curves obtained with this method are shown in Fig.4.6. It was observed that there is no plateau region in the plot of T_m, but rather very slow increases at the beginning of the plot up to ≈260°C and then a quick increase up to T_{stop}=380 °C are noticeable.

A similar behavior was also observed for T_1 and T_2, but the increase in the slope of T_1 is always faster than T_2. This situation indicates that the FWHM and half-width on the high temperature side of the peak maximum (δ=T_2−T_m) of the

dosimetric peak of CaF_2:Mn are not constant, but rather change with T_{stop} as shown in Fig.4.7(a).

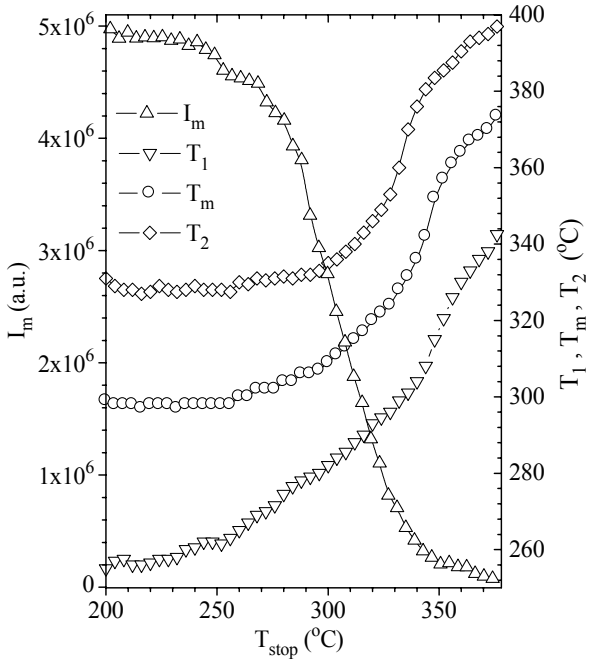

Figure 4.6 T_1–T_{stop}, T_m–T_{stop}, T_2–T_{stop} and I_m-T_{stop} plot for the thermoluminescent dosimetric glow peak of CaF_2:Mn

It was also observed that the calculated values of the geometric factor μ_g of this peak always increases from 0.42±0.01 to 0.56±0.02 with increasing T_{stop} up to 335 ^oC but the variation is highly effective above T_{stop}>300 °C. And then it quickly decreases to 0.43±0.01 up to 355 ^oC and above that point it becomes approximately stable at around 0.43±0.01 up to T_{stop} = 380 °C (Fig.4.7(a)). The process of thermal quenching of luminescence might be one of the causes of the change in μ_g value depending on the value of T_{stop}, since the process of thermal quenching affects the form of the glow curve due to its non-linear dependence on temperature.

Another reason might be that the dosimetric peak consists of several first- and/or general-order glow peaks and the decrease in the intensity of prior component becomes more efficient with increasing stopping temperature than the other. Then, these could affect the μ_g value of the whole peak. The recorded glow curves after the T_m–T_{stop} experiment were also used to determine the activation energy of dosimetric glow peak in the glow curve of CaF_2:Mn by the PS method. The plots of calculated activation energies by the PS method are shown in Fig.4.7 (b). Note that the dosimetric peak was always assumed to be a single peak during the calculation of E_a in this experiment.

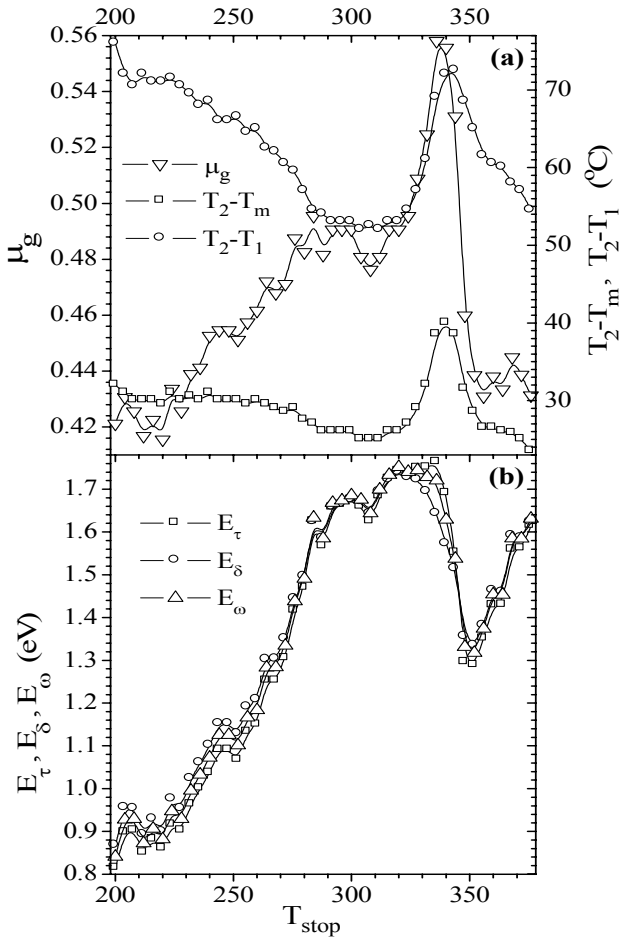

Figure 4.7 (a) The geometric factor μ_g , T_2-T_1 and T_2-T_m as a result of T_{stop} determined from the T_m–T_{stop} procedure. Lines are fits to guide the eye (D≈4.5 Gy). (b) The activation energy (E_a) resulting from the PS method after the T_m–T_{stop} procedure

In some cases, if the glow curve structure has highly overlapping glow peaks, the number of glow peaks might be better figured out with a plot of E_a against T_{stop} instead of from the T_m–T_{stop} plot. Therefore, the IR method was also employed to obtain the E_a–T_{stop} plot in this work. This method is one of the most reliable methods for evaluating E_a of a single glow peak. In this method, at the beginning of the TL glow peak, the concentration of trapped electrons n_o changes by only a small amount with temperature and thus it can be regarded as constant, so that the first- and general-order TL equations are simplified as $I(T) \alpha A \exp(-E_a/kT)$, where A is a constant and the TL intensity is independent of b. Therefore, a plot of $\ln(I)$ versus $1/T$ would yield a straight line with a slope of $-E_a/k$, from which E_a can readily be calculated. This method can be used only in the initial region of the TL signal up to ≈10% of its peak maximum (I_m). However, if the intensity at the beginning of each

peak is very low and especially when the glow curve is composed of several glow peaks, the obtained values of E_a may not reflect the actual values.

Therefore, in such a case, the values of E_a obtained by the IR method often need corrections. Christodoulides [48] and Singh *et al* [49] have proposed the use of high level of glow peaks to reduce the inaccuracies in E_a due to high levels of the used signal, which was also utilized in this work. Another issue during the evaluation of E_a by IR is the effect of thermal quenching effect on the evaluated E_a. This effect underestimates the values of E_a obtained by the IR method. Since the experimental glow curve shape is highly distributed by the thermal quenching effect, it cannot give reliable information about the values of E_a. However, the IR method analyses only the leading part of the glow peak and as such yields data appropriate to only that component of the TL signal comprising the full peak. Therefore, even if the IR method gives erroneous values of E_a when thermal quenching is present in the material, it should be expected that the plot of E_a against T_{stop} still gives plateau regions with a gradual decrease at the end of each plateau after the T_m–T_{stop} procedure even if the glow curve is the superposition of overlapping glow peaks. It is well known that the thermal quenching effect is dominant around the TL dosimetric peak of CaF_2:Mn [50,51]. Therefore, the reduction of E_a values was clearly observed by previous researches in this field [52, 53]. The result of calculated activation energies is shown in Fig. 4.8 as a function of T_{stop}. As seen in this figure, the E_a values quickly increase from 1.6±0.01 to 1.68 ± 0.02 eV between 200 °C and 215 °C. This increase is probably due to the diminishing of the satellite peaks from the low temperature side of dosimetric peak with increasing T_{stop}. After the complete annihilation of these peaks from the glow curve when T_{stop}>215 °C, the calculated E_a values become nearly constant around 1.68±0.01 eV, which is believed to give the E_a of first glow peak in the dosimetric glow peak. Beyond 260 °C, after a very slight increase, the values of E_a again become nearly constant around 1.72±0.01 eV, which gives the E_a value of the other glow peak (peak 2) up to T_{stop}≈290 °C. At the end of the flat region of this peak, the E_a values again become constant near 1.74±0.01 eV which give the E_a value of another peak (peak 3) up to 310 ˚C. These values agree well with the known value of activation energy E_a≈1.73 eV in previously published studies determined from the initial part of the TL peak [54]. After the complete vanishing of this peak, the calculated values of the activation energies were continuously decreased between 1.73 and 1.66 eV up to 330 °C. No flat regions were

noticed around this region. At the end of this region, the calculated values of E_a quickly decrease from 1.66 to 1.44±0.01 eV with increasing T_{stop} and another plateau was again obtained near 1.44±0.01 eV between 340 ^oC and 360 ^oC and it was deduced that this flat region gives the activation energy of peak 5 by the IR method. No flat regions were noticed after that region. Hence, we can say that the process of thermal quenching should be effectively revealed when T_{stop} exceeds 310 °C.

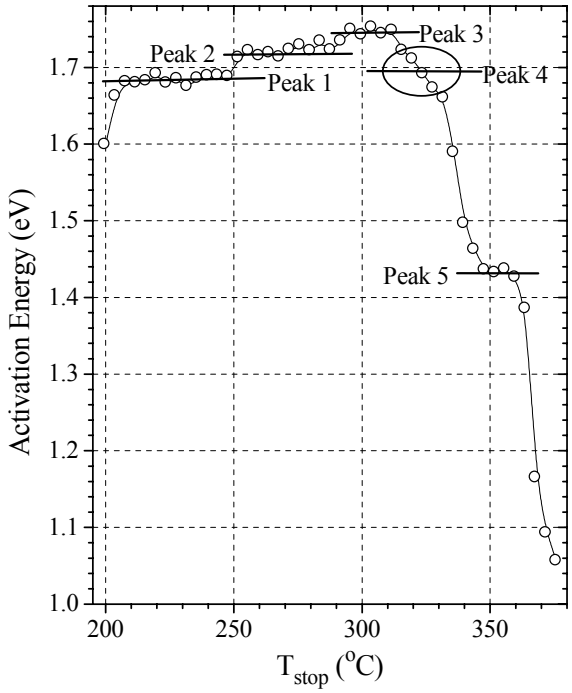

Figure 4.8 The activation energy (E_a) resulting from the RIR method after T_m–T_{stop} procedure

4.1.4. Glow curves analysis by CGCD method

The all glow curves were also analyzed by CGCD method to obtain the number of glow peaks. This method has become very popular to obtain the number of glow peaks in the complex glow curves and their kinetic parameters for the last three decades [16]. It is apparent that if the number of data points used in the analysis increases, the potential for accurate evaluation of number of glow peaks and their kinetic parameters gets better. Therefore, this method has great advantages over methods. However, it must be noted that different models, approximations and minimization procedures are used for the glow curve analysis in the CGCD program. As a consequence, one may wonder whether the results of CGCD method reflect the accurate kinetic parameters of the TL peaks. According to many experienced researchers, the results obtained by the CGCD method, in some cases, seem to be

unreliable. Especially, the advantages of the CGCD method may be undermined in complex TL glow curves. As a result, many possible sets of kinetic parameters could be assigned to the same glow curve if different number of glow peaks was used in the CGCD program. Therefore, the number of gow peaks was only investigated by the CGCD method in the given study. The used CGCD program, which is based on the least square minimization procedure, was developed at the Reactor Institute at Delft, The Netherlands [55]. In this study, the first-order kinetics were approximated for all CGCD evaluations by the expression [52, 53]:

$$I(T) = n_0 s \exp(-\frac{E}{kT}) \exp\left[-\frac{s}{\beta}\frac{kT^2}{E}\exp(-\frac{E}{KT}) * (0.992 - 1.620\frac{kT}{E}) \right] \qquad (1)$$

and the general-order kinetics were approximated by the expression

$$I(T) = n_0 s \exp(-\frac{E}{kT})\left[1 + \frac{(b-1)s}{\beta}\frac{kT^2}{E}\exp(-\frac{E}{kT}) * (0.992 - 1.620\frac{kT}{E}) \right]^{\frac{b}{1-b}} \qquad (2)$$

where n_0 (m^{-3}) is the number of trapped electrons at t = 0, k (eVK^{-1}) is the Boltzman's constant. Other parameters are as described earlier. The goodness of fit for all the measured glow curves was tested using the figure of merit (FOM) [56]. From many experiences, it can be said that, if the values of the FOM are between 0.0% and 2.5% the fit is good, between 2.5% and 3.5% is a fair fit, and >3.5% is a bad fit. Detailed information on the deconvolution method has been given elsewhere [16].

The number of glow peaks is not a free fitting parameter during the deconvolution of the measured glow curve into individual components in the CGCD programs. If the number of peaks is not known, it can be found by fitting the glow curve several times with a different number of components up to obtaining best-fit result. Therefore, the real number of glow peaks to be in the glow curve of CaF_2:Mn was investigated by using different number of glow peaks in the CGCD program. In previously published studies [9-13], it was observed that there are some conflicts regarding the number of glow peaks and, therefore, there is no consensus on this parameter up to now. In the given study, it was observed that it is not possible to fit the dosimetric peak of CaF_2:Mn by two and three components with first and/or general-order kinetics. Moreover, there were large differences between experimental and computed glow curves when four first-order components were assumed in the

CGCD program. Nevertheless, the goodness of fit was relatively improved compared to the fitting by three first or general-order components. In this study, after many tries with different number of glow peaks, it was observed that the glow curve structure of CaF_2:Mn is well described by a linear combination of at least five first-order glow peaks. In this case, a reasonably good fit was always obtained. Therefore, the dosimetric peak of CaF_2:Mn was always fitted with five first-order components**.** Some of the CGCD analyzed TL glow curves of CaF_2:Mn irradiated after different dose levels, given in the caption of the figure, are shown in Fig. 4.9 along with their components.

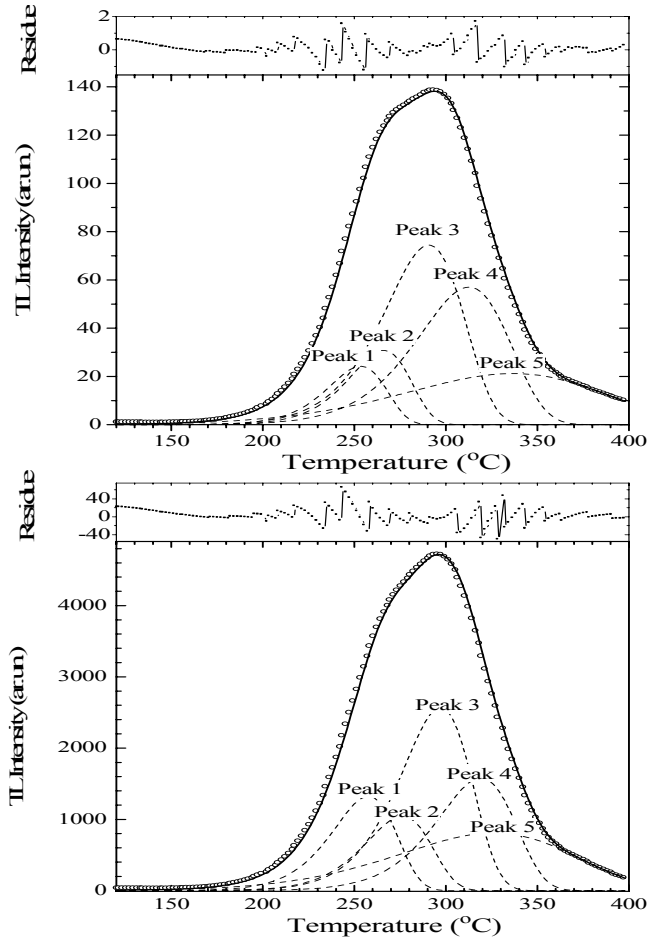

Figure 4.9 Some of the CGCD analyzed glow curves after various dose levels. (*a*) $D \approx 0.12$, (*b*) $D \approx 3.85$ Gy. In all figures, open circles, solid lines and dotted lines represent the experimental points, global fitting and fitted individual peaks, respectively ($\beta = 1$°C s^{-1}*)*

In the present study, the influence of heating rates between 1 and 20 °C s^{-1} on the response of dosimetric glow peaks of CaF_2:Mn (TLD-400) and its dose response characteristic were also investigated by the peak height and peak area methods using

CGCD technique. A possible temperature lag between the heating planchet and the TL sample was minimized using thermally conductive non-luminescent silicon oil between the heating planchet and the sample. A set of glow curves measured with different heating rates is shown in Fig. 4.10. The influence of heating rate on the glow peaks is clearly seen in this figure. As espected in theory, the peak temperatures of all peaks in the glow curves of CaF2:Mn are shifted higher side as the heating rate increases. But the rate of shifting is decreased with increasing heating rate. On the other hand, both peak intensities and total area of dosimetric glow peak continuouslydecrease with increasing heating rate in the investigated heating rate region. Moreover, the influence of heating rates on the intensities of glow peaks is highly different from each other. As seen, the influence of the heating rates on the intensities of glow peaks becomes more effective with increasing peak temperatures of glow peaks.

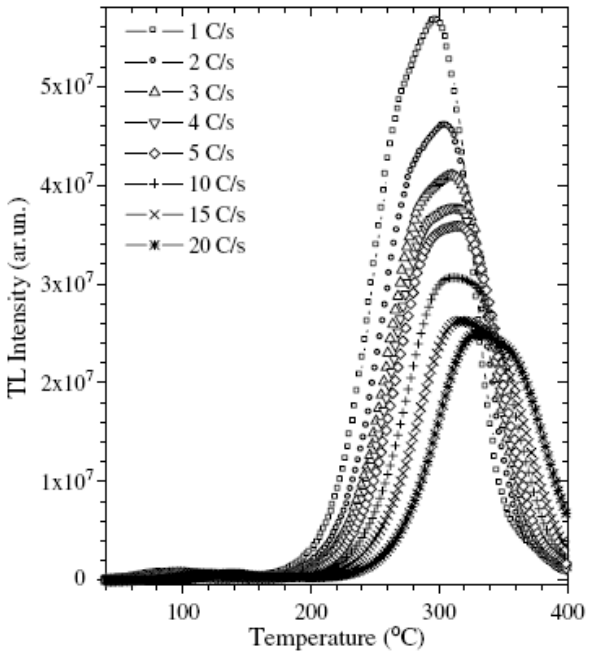

Figure 4.10 Some of the selected glow curves of CaF_2:Mn measured at various heating rates from 1°Cs^{-1} to 20°Cs^{-1}. All the glow curves were measured after β-irradiation to a dose level of ≈4.5 Gy

The results of CGCD analyses plus the peak height of dosimetric glow peak of TLD-400 are shown in Fig.4.11. In this figure, the TL responses of glow peaks are normalized at the lower heating rate (1 °C s^{-1}). The observed variations in the integrated areas of glow peaks with heating rate using the CGCD method are

complicated. The irregular variations on the peak integrals of glow peaks appear to be due to the artificial effects of the CGCD method. Therefore, the integrated areas of combined peaks (1 + 2 and 3 + 4 + 5) and whole area of dosimetric glow peak were shown instead of the individual peak areas in the given study. As seen from Fig. 4.11, despite the decrease in the integrated area of the combined peaks 1 + 2 by about 20-30 % with heating rates from 1 to 20 °C s^{-1} , the integrated area of combined peaks 3 + 4 + 5 is on the order of 65 %, and whole area of dosimetric glow peak is at around 50%. It was evaluated that the decrease in the peak height intensity is the order of 55%.

Two mechanisms have been suggested in the literature to explain the decrease in the luminescence efficiency, and both give rise to an expression of the form of $\eta = (1 + C\exp(-W / kT))^{-1}$, where W and C are the quenching parameters. In the former, the reduction in intensity of TL peaks can be attributed to the thermal quenching effect. The thermal quenching of luminescence was first observed in natural quartz [2]. It was understood to due to the increased probability of nonradiative transitions competing with radiative transitions. In fact, the luminescence efficiency of a phosphor is given by $\eta = P_r / (P_r + P_{nr})$, where P_r is the probability of luminescence transitions, temperature independent and P_{nr} is the probability of nonradiative transitions, which is temperature dependent. Since the increase in the heating rate resulted in an increase in the temperature of the TL glow peak, this shift in temperaturewas held responsible for the increase in the contribution of non-radiative transitions. Then, it was infered that the glow peaks occurring at higher temperatures must exhibit higher thermal quenching than those occurring at lower temperatures any TLD material. Apart from the increased probability of nao-radiative transitions at higher temperatures, the observed effects have also been assigned to the effects of heating rate on the migration of charge carriers released during the TL readout. If the lattice parameters are responsible for the non-radiative transitions, the increase in the mobility of the cherge carriers with temperature would reduce the luminescence efficiency and therefore the responce will reduce at a faster heating rate. However, in order to have a tenable explanation for the variation of peak intensities with the heating rate, it will require a more detailed investigation because a single model may not be sufficient to explain the

observed variations and many models can play a role in the variations of TL responce of this material.

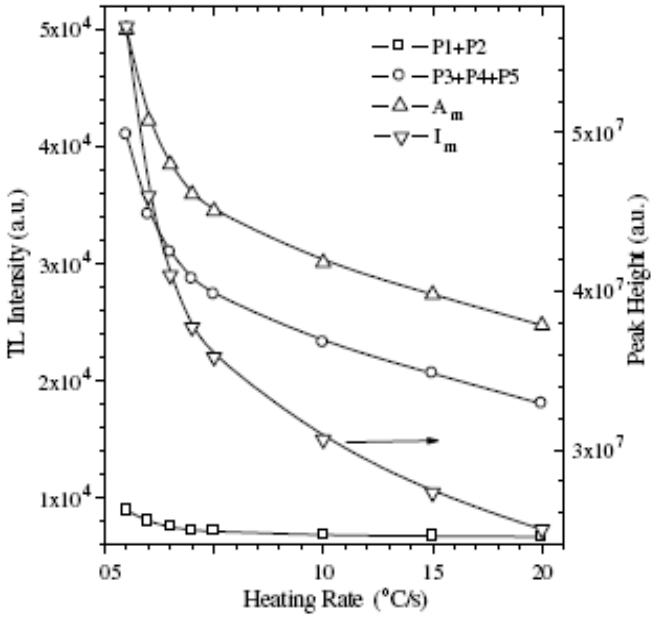

Figure 4.11 Deconvoluted TL response of combined glow peaks of TLD-400 as a function of heating rate. The integral of each graph was normalized at the lower heating rate (1 $^{\circ}Cs^{-1}$). I_m shows the peak value of dosimetric glow peak of TLD-400. Dose level (D) ≈4.5 Gy

The kinetic parameters of CaF_2:Mn were also analyzed by the CGCD method after different heating rates. It was observed that they are not constant but vary irregularly with heating rates. Therefore, the obtained results were not given in the present study. One of the possible explanations of this event is the artificial effects of the CGCD method on the evaluated kinetic parameters. As mentioned previously, a small change in the intensity of dosimetric peak should increase the artificial effects of the CGCD method on the kinetic parameters of all glow peaks evaluated by it. Therefore, some of the advantages of the CGCD method become offset, because small distortions in the glow curve yield erroneous trapping parameters as the computerized curve fitting routine attempts to define the 'best-fit' to the numerical data.

Some of the selected glow curves after different dose levels are shown in Fig.12. All data in dose response are plotted on a log–log scale and shown in figure 12. It is clearly seen that the obtained dose responses of dosimetric glow peak by peak height and area methods follow similar pattern. They are a little bit superlinear

between ≈0.015 Gy and ≈110 Gy with slightly different slopes. The calculated values of slopes from peak height and area methods are 1.037 and 1.021 on the log-log scale, respectively. In general, the two types of models are usually employed for explaining the superlinearity of dose TL [57]. One involves competition during excitation between trapping states, which causes the filling of the relevant trap or center to be superlinear. The other model deals with competition during heating which may result in a strong superlinearity, even if the filling of the trap and center in question are linear with the dose. In the present work, it is thought that both of the processes can take place in the studied material but further work along these lines are needed to explain this event in TLD-400.

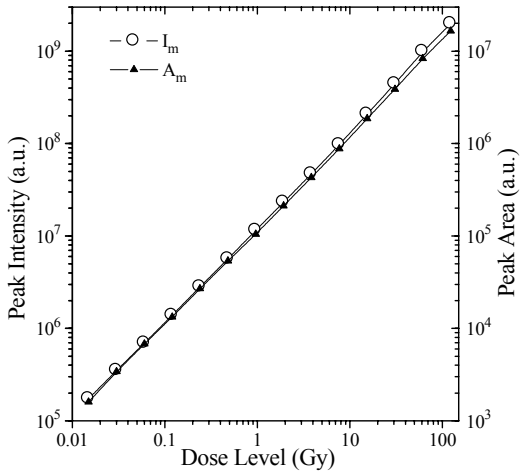

Figure 4.12 The TL dose response curve of dosimetric glow peak in the glow curve of CaF_2:Mn sample determined by the peak height and area of glow peak

CHAPTER 5

CONCLUSION

The results in this work indicate that the reproducibility of deconvoluted area of dosimetric peak of CaF_2:Mn is highly depend upon the annealing temperature, time and preceding dose level applied to the dosimeter before usage. The additive dose method indicates that the position of the dosimetric peak does not shift towards lower or higher temperature sides with increasing dose level (Figs.4.2 and 4.3), while its geometric shape factor (μ_g) changes with dose levels. Additionally, the T_m–T_{stop} procedure indicates that the position of dosimetric peak shifts towards the high temperature side with increasing T_{stop}. These results imply that the dosimetric peak of CaF_2:Mn after β-irradiation can be best described as a superposition of glow peaks. A detail analysis of this peak with the AD, E_a-T_{stop}, and CGCD methods indicate that all of them have first-order kinetics. The results of AD experiments were also indicated that the kinetic parameters of these peaks are dependent on the dose level. After the application of T_m–T_{stop} procedure and completely annihilation of low temperature satellite peaks from the glow curves with increasing stopping temperature, the determined kinetic parameter values found by IR, CGCD and PS methods for the P_3, P_4, and P_5 approach to each other and they reach 1.6±0.1 eV. However, there is no any consensus or agreement between the results before the application of T_m–T_{stop} procedure. One possible explanation for the confliction on the value of kinetic parameters is that the variation in the emission spectrum with temperature, self-absorption, thermal quenching and application of a high heating rate are some possibilities for causing distortions in the glow curve shape which in turn have an effect on the evaluated kinetic parameters of Mn-doped CaF_2 crystal. Additionally, a distribution of activation energies and frequency factors may cause a variation of the estimated kinetic parameters.

REFERENCES

[1] Ronogajec-Komor, M. (2002). Thermoluminescence dosimetry-Appliction in Monitoring. *Radiation Safety Management*, **2** (1), 2-16.

[2] McKeever, S. W. S. (1985). Thermoluminescence of Solids, (Cambridge: Cambridge University Press).

[3] Zarate-Morales, A. Buenfil, A. E. (1996). Environmental Gamma Dose Measurements in Mexico City Using TLD. *Health Physics*, **71**(3), 358-361.

[4] Kalchgruber, R. Göksu, H. Y. Hochhäuser, E. Wagner, G. A. (2002). Monitoring environmental dose rate using Risø TL/OSL readers with built-in sources: Recommendations for users. *Radiat. Meas.*, **35**, 585-590.

[5] Chakrabarti, K. Sharma, J. Mathur, V. K. (1993). Laser Bleaching of Deep Traps and Reduction of Zero Dose Problem in CaF_2:Mn Dosemeters. *Radiat. Prot. Dosim*., **47**,155-158.

[6] Joanne, F. Rhodes, R. J. Abbundi, D. Wayne Cooke, V. K. Mathur, M. D. Brown, (1985). Temperature dependence of fluorescence spectra from x-ray-excited single-crystal CaF_2:Mn(x) (x=0.1, 1.0, 3.0 at. %). *Phys. Rev. B*, **31**, 5393-5398.

[7] McMasters, D. W. Jassemnejad, B. McKeever, S. W. S. (1987). Some observations regarding the effects of background rare-earth impurities on the thermoluminescence and optical absorption of CaF_2:Mn. *J. Phys. D: Appl. Phys.*, **20**, 1182-1190.

[8] Chakrabarti, K. Sharma, J. Mathur, V. K. Barkyoumb, J. H. (1995). Optical properties of radiation defect centers involving single and paired Mn^{2+} centers in CaF2:Mn. *Phys.Rev.B:Condevs Matter*., **51**(23), 16541-16548.

[9] Allen, P. McKeever, S. W. S. (1990). Studies of PTTL and OSL in TLD-400. *Radiat. Prot. Dosim*., **33**, 19-22.

[10] Paul, W. Levy. (1985). Recent developments in thermoluminescence kinetics. *Nuclear Tracks and Radiation Measurements*, **10**(1-2), 21-32.

[11] Hornyak, W. F. Levy, P. W. Kierstead, J. A. (1985). CaF_2:Mn thermoluminescence: A single glow peak not described by 1st or 2nd order kinetics. *Nuclear Tracks and Radiation Measurements,* **10**(4-6), 557-563.

[12] Hsiang-En, W. Shan-Wen, L. Pao-Shan, W. Pin-Chieh, H. (1995). A Study of the Main Glow Peak for CaF_2:Mn. *Applied Radiation and Isotopes*, **46**(9), 869-873.

[13] Drazic, G. Miklavzic, U.Mihelic, M. (1986). The Influence of TL Glow Curve Evaluation Algorithms on the Reproducibility of Dosemeter Readings. *Radiat. Prot. Dosim*., **17**, 343-346.

[14] Jassemnejad, B. McKeever, S. W. S. Abbundi, R. J. Mathur, V. K. Brown, M. D. (1986). Optical Absorption and Thermoluminescence in Calcium Fluoride Doped with Manganese and Cerium. *Radiat Prot Dosimetry*, **17**, 469-473.

[15] Mathur, V. K. Abbundi, R. J. Brown, M. D.McKeever, S. W. S. (1986). Radiation Induced Defects in Mn-doped CaF_2. *Radiat. Effects*, **99**, 10-14.

[16] Horowitz, Y.S. Yossian, D. (1995). Computerised Glow Curve deconvolution: Application to thermoluminescence Dosimetry Monograph. *Radiat. Prot. Dosim.,* **60**, 1-115.

[17] Mahesh, K. Weng, P. S. Furetta, C. (1989). *Thermoluminescence in Solids and its Applications* (Ashford: Nuclear Technology Publishing).

[18] Chen R. McKeever, S.W.S. (1997). Theory of Thermoluminescence and Related Phenomena. *World Scientific Publications*, London, NJ, Singapore, 576pp.

[19] Chen, R. Kirsh, Y. (1981). *Analysis of Thermally Stimulated Processes,* (Oxford: Pergamon), 361 pp.

[20] Daniels, F. Boyd, C.A. Saunders, D.F. (1953). *Science,* **117**, 343.

[21] Townsend P. D. Kelly, J. C. (1993). Colour Centres and Imperfections in Insulators and Semiconductors. *Sussex University Press*, London.

[22] McKeever, S.W.S. Moscovitch, M. Townsend, P. D. (1995). *Thermoluminescence Dosimetry Materials: Properties and Uses*, Nuclear Technology Publishing, Kent.

[23] Randall, J. T. Wilkins, M. H. F. (1945). *Proc. R. Soc. London Ser. A,* **184**, 366.

[24] Randall, J. T. Wilkins, M. H. F. (1945). *Proc. R. Soc. London Ser. A,* **184**, 390.

[25] Chen, R., in: Y. S. Horowitz (Ed.). (1984). *Thermoluminescent and Thermoluminescent Dosimetry*, Vol. 1, CRC Press, Boca Raton, FL.

[26] Kitis, G. Gomez-Ros, J. M. Tuyn, J. W. N. (1998). *J. Phys. D: App. Phys.,* **31**, 2636.

[27] Pagonis, R. V. Mian, S. M. Kitis, G. (2001). *Radiat. Protect. Dosim*., **93**, 11.

[28] Garlick G. F. J. Gibson, A. F. (1948). *Proc. Phys. Soc.,* **60**, 574.

[29] Bos, A. J. J. Dielhof, J. B. (1991). The Analysis of Thermoluminescent Glow Peaks in CaF_2:Tm (TLD-300). *Radiat. Prot. Dosim.,,* 37, 231-239.

[30] May, C. E. Partridge, J. A. (1964). *J. Chem. Phys*. **40**, 1401.

[31] Chen, R. Winer, A.A (1970). *J. Appl. Phys*., **41**, 5227.

[32] Piters, T. M. Bos, A. J. J. (1993). *J. Phys. D: Appl. Phys*., **26**, 2255.

[33] Chen, R. (1969). *J. Appl. Physics,* **40**, 570.

[34] Grossweiner, L. I. (1953). *J. Appl. Physics,* **24**, 1306.

[35] Halperin, A. Braner, A. A. (1960). *Phys. Rev*., **117**, 405.

[36] Booth, A. H. (1954). *Can. J. Chem*., **32**, 214.

[37] Azerin, J. (1986). *Nucl. Tracks,* **11**, 159.

[38] Bunghkbardt, B. Singh, D. Piesch, E. (1977). *Nuclear Instrumentations and Methods*, **142**.

[39] Kathuria, S. P. Sunta, C. M. (1979). *J. Phys. D: Appl. Phys*.,**12**, 1573.

[40] Bos, A. J. J. Piters, T. M. Go´mez-Ros, J. M. Delgado, A. (1993). (GLACANIN, and Intercomparision of Glow Curve Analysis Computer Programs) IRI- CIEMAT Report 131-93-005 IRI Delft

[41] Hsu, P. C. Wang, T. K. (1984). *Radiat. Protect. Dosim*., **16**, 253.

[42] Sunta, C. M. (1984). *Radiat. Protect. Dosim*., **8**, 25.

[43] Kitis, G. Furetta, C. Prokic´, M. Prokic´, V. (2000). Kinetic parameters of some tissue equivalent thermoluminescence materials. *J. Phys. D: Appl. Phys.,* **33,** 1252.

[44] Furetta, C. Kitis, G. Kuo, C.H. (2000). Kinetics parameters of CVD diamond by computerised glow-curve deconvolution (CGCD). *Nucl. Instr. and Meth. B,* **160**, 65.

[45] Yossian, D. Horowitz, Y.S. (1995). Computerized glow curve deconvolution applied to the analysis of the kinetics of peak 5 in LiF:Mg, Ti (TLD-100). *J. Phys. D. Appl. Phys.* **28,** 1495.

[46] Yazici, A.N. Chen, R. Solak, S. Yegingil, Z. (2002). The analysis of thermoluminescent glow peaks of CaF2:Dy (TLD-200) after birradiation. *J. Phys. D: Appl. Phys.,* **35**, 2526.

[47] Chen, R. (1969). Glow curves with general order kinetics. *J. Electrochem. Soc.,* **116**, 1254.

[48] Christodoulides, C. (1985). Errors involved in the determination of activation energies in TL and TSDC by the initial rise method. *J. Phys. D: Appl. Phys.,* **18**, 1665.

[49] Singh, T.S.C. Mazumdar, P.S. Gartia, R.K. (1988). On the determination of activation energy in thermoluminescence by the initial rise method. *J. Phys. D: Appl. Phys.,* **21,** 1312.

[50] Gorbics, S.G.. Nash, A.E Attix, F.H. (1969). Thermal quenching of luminescence in six thermoluminescent dosimetry phosphors – II: quenching of thermoluminescence. *Int. J. Appl. Radiat. Isotopes,* **20** (12), 843.

[51] Pradhan, A.S. (2002). Effect of heating rate on the responses of CaF2:Cu, CaF2:Tm, CaF2:Dy and CaF2:Mn. *Radiat. Prot. Dosim.,* **100,** 289.

[52] Necmeddin Yazici, A. Solak Semra, Öztürk Zihni, Tokasu Mustafa, Yegingil Zehra, (2003). The analysis of dosimetric glow peak of a-Al2O3:C after different dose levels by β-irradiation. *J. Phys. D : Appl. Phys.,* **36** (2), 181.

[53] Necmeddin Yazici, A. Topaksu Mustafa, (2003). The analysis of thermoluminescence glow peaks of unannealed synthetic quartz. *J. Phys. D: Appl. Phys.*, **36** (6), 620.

[54] Zahedifar, M. (2003). Study on dosimetry peak and trapping parameters of CaF2 :Mn(TLD-400) thermoluminescence dosimeters, in: 5th European Conference on Luminescent Detectors and Transformers of Ionizing Radiation; September 1–5, Prague.

[55] Bos, A.J.J. Piters, T.M. Go´mez-Ros, J.M. Delgado, A. (1993). An intercomparison of glow curve analysis computer programs: I. Synthetic glow curves. *Radiat. Prot. Dosim.,* **47,** 473.

[56] Misra, S.K. Eddy, N.W. (1979). A formula for universal assessment of goodness-of-fit of gamma ray spectra. *Nucl. Instr. and Meth.*, **166**, 537.

[57] Chen, R. Fogel, G. Lee, C.K. (1996). A new look at the models of the superlinear dose dependence of thermoluminescence. *Radiat. Prot. Dosim.,* **65**, 63.

[58] A. Necmeddin Yazıcı, Metin Bedir, A. Sibel Sökücü (2007). The analysis of dosimetric thermoluminescent glow peak of CaF2:Mn after Beta-irradiation*., Nuclear Instruments and Methods in Physics Research B,* **259,** 955–965.